UNIVERSIDADE ESTADUAL PAULISTA
"JÚLIO DE MESQUITA FILHO"
Instituto de Biociências
Câmpus do Litoral Paulista

Integração de genômica de populações e modelagem biofísica de dispersão por correntes oceânicas para inferência da conectividade de árvores de mangue do litoral brasileiro

ANDRÉ GUILHERME MADEIRA

SÃO VICENTE – SP
2022

Instituto de Biociências - Câmpus do Litoral Paulista
Praça Infante D. Henrique s/nº - CEP 11330-900 - São Vicente (SP) - Brasil
Tel. (13) 3569-7100 - Fax (13) 3569-7146 - diretor.clp@unesp.br

UNIVERSIDADE ESTADUAL PAULISTA
"Júlio de Mesquita Filho"

INSTITUTO DE BIOCIÊNCIAS CÂMPUS
DO LITORAL PAULISTA

Integração de genômica de populações e modelagem biofísica de dispersão por correntes oceânicas para inferência da conectividade de árvores de mangue do litoral brasileiro

André Guilherme Madeira

Orientador: Dr. Gustavo Maruyama Mori

Dissertação apresentada ao Instituto de Biociências, Câmpus do Litoral Paulista, UNESP, para obtenção do título de Mestre no Programa de Pós-Graduação em Biodiversidade de Ambientes Costeiros.

SÃO VICENTE - SP
2022

M181i

Madeira, André Guilherme

Integração de genômica de populações e modelagem biofísica de dispersão por correntes oceânicas para inferência da conectividade de árvores de mangue do litoral brasileiro / André Guilherme Madeira. -- São Vicente, 2022

58 p. : il., tabs.

Dissertação (mestrado) - Universidade Estadual Paulista (Unesp), Instituto de Biociências, São Vicente

Orientador: Gustavo Maruyama Mori

1. Genética da paisagem marinha. 2. Dispersão. 3. Rhizophoraceae. 4. RADseq. 5. Taxas de migração. I. Título.

Sistema de geração automática de fichas catalográficas da Unesp. Biblioteca do Instituto de Biociências, São Vicente. Dados fornecidos pelo autor(a).

Essa ficha não pode ser modificada.

Agradecimentos

Primeiramente, ao meu orientador, Gustavo, que ao longo desses últimos anos se tornou meu amigo e companheiro profissional. Aprendo todos os dias contigo a como ser um ótimo professor, pesquisador e orientador. Muito obrigado pelo companheirismo, pela paciência, pela amizade, por acreditar em mim e por abrir portas para oportunidades incríveis de crescimento.

À banca examinadora da qualificação, Dra. Prianda Laborda, Dra. Sónia Andrade e Dr. Alison Nazareno, e da defesa, Dr. Marcelo Kitahara e Dr. Evandro Marsola pelos valiosos comentários e pela contribuição indispensável ao nosso trabalho.

Aos companheiros do laboratório de Ecologia Molecular, que contribuíram com as sugestões para a apresentação e com as reuniões de laboratório. Às minhas companheiras e aos meus companheiros da pós-graduação Vitor, Natália, Samantha, Marcelo e Vitória, que encararam comigo um mestrado à distância e compartilharam das dificuldades e desafios desse período, tornando tudo um pouco mais leve.

À Mayumi, por dividir a casa (e o Gohan) comigo nesse último ano e se tornar uma grande amiga e irmã.

À minha companheira, Cris, que me deu o suporte necessário o tempo todo para a conclusão desse capítulo, por me encorajar, me apoiar e fazer de tudo para tornar essa etapa mais prazerosa e especial.

À minha família, que sempre foi um porto seguro para o qual retornar e sempre comemorou demais minhas conquistas.

Às funcionárias e funcionários da Unesp Campus do Litoral Paulista e às professoras e professores do programa de pós-graduação em Biodiversidade de Ambientes Costeiros.

À FAPESP, pelo apoio financeiro por meio das bolsas de pesquisa FAPESP 2017/12920-8, 2018/02655-8 e 2020/07967-8 ao longo dos últimos anos. O presente trabalho foi realizado com apoio da Coordenação de Aperfeiçoamento de Pessoal de Nível Superior - Brasil (CAPES) - Código de Financiamento 001.

A todas e todos que lutam pelo futuro da ciência e da educação no nosso país.

Sumário

Resumo

A dispersão é um mecanismo crucial, permitindo que populações e espécies possam alcançar novos recursos e explorar novas condições ambientais. No entanto, descrever mecanismos de dispersão de espécies que podem estar distribuídas por grandes áreas pode ser custoso ou mesmo inviável, como é o caso para as árvores de mangue. A influência das correntes oceânicas na dispersão dos propágulos de mangue tem sido cada vez mais evidente; entretanto, poucos estudos relacionam mecanisticamente os padrões de distribuição populacional com a dispersão pelas correntes oceânicas de forma integrada. Nesse trabalho, avaliamos o papel das correntes oceânicas na dispersão e conectividade do mangue vermelho, *Rhizophora mangle*, ao longo da costa do Sudoeste do Atlântico. Inferimos a estrutura populacional as taxas de migração a partir de polimorfismos de base única, simulamos o deslocamento de propágulos ao longo da região do Sudoeste do Atlântico e testamos nossas hipóteses com testes de Mantel e análise de redundância. Observamos uma estrutura genética de populações composta por dois grupos, norte e sul, que é corroborada por outros estudos com *R. mangle* e outras plantas costeiras. As taxas de migração recentes inferidas não indicaram migração atual entre os locais amostrados. Por outro lado, inferências de migração históricas demonstraram baixas taxas de migração entre os grupos e padrões de dispersão diferentes para cada um deles, o que está de acordo com o esperado para eventos de dispersão a longa distância. Nossos testes de hipóteses sugerem que tanto o isolamento por distância quanto o isolamento por resistência (derivado das correntes oceânicas) podem explicar a variação genética neutra de *R. mangle* na região. Nossas descobertas expandem o conhecimento atual sobre conectividade de mangues e revelam como a combinação de evidências moleculares e modelagens oceanográficas ampliam a capacidade de interpretação do processo de dispersão, que têm implicações ecológicas e evolutivas.

Palavras-chave: Rhizophoraceae, RADseq, LDD, genética da paisagem marinha, taxas de migração.

Abstract

Dispersal is a crucial mechanism to living beings, allowing them to reach new resources such that populations and species can explore new environment conditions. However, describing dispersal mechanisms of widespread species can be costly or even impracticable, which is the case for mangrove trees. The influence of ocean currents on the mangroves' propagules' movement has been increasingly evident; however, few studies mechanistically relate the patterns of population distribution with the dispersal by oceanic currents under an integrated framework. Here, we evaluate the role of oceanic currents on dispersal and connectivity of *Rhizophora mangle* along the Southwest Atlantic basin. We inferred population genetic structure and migration rates based on single nucleotide polymorphisms, simulated the displacement of propagules along the Southwest Atlantic coast and tested our hypotheses with Mantel tests and redundancy analysis. We observed a two populations structure, north and south, which is corroborated by other studies with *Rhizophora* and other coastal plants. The inferred recent migration rates do not indicate gene flow between the sampled sites. Conversely, long-term migration rates were low across groups and contrasting dispersal patterns within each one, which is consistent with long-distance dispersal events. Our hypothesis tests suggests that both isolation by distance and isolation by oceanography (derived from the oceanic currents) can explain the neutral genetic variation of *R. mangle* in the region. Our findings expand the current knowledge of mangrove connectivity and highlight how the association of molecular methods with oceanographic simulations improve the interpretation power of the dispersal process, which has ecological and evolutionary implications.

Keywords: Rhizophoraceae, RADseq, LDD, seascape genetics, migration rates.

Introdução Geral

Mangues e manguezais

Os mangues são plantas lenhosas – árvores e arbustos – altamente especializadas, de diversos gêneros derivados de ao menos 27 linhagens independentes que apresentam adaptações convergentes para a vida em regiões tropicais e subtropicais entre marés (He et al., 2022; Tomlinson, 2016). Esses ambientes são caracterizados pela influência das marés, hipóxia, substrato inconsolidado, altas taxas de radiação UV, de modo que mangues desenvolveram adaptações morfológicas e fisiológicas a essas condições durante sua evolução, como raízes respiratórias expostas (pneumatóforos), raízes de suporte e folhas excretoras de sal (Kathiresan & Bingham 2001; Tomlinson 2016). Entre essas adaptações, encontram-se os propágulos; unidades dispersoras – frutos ou sementes – que são capazes de permanecer por semanas ou meses no mar, sem perder sua viabilidade (Tomlinson, 2016; Van der Stocken, Wee, et al., 2019), o que faz com que as árvores de mangue sejam capazes de se dispersar por milhares de quilômetros.

Essa ampla capacidade de dispersão está associada com a distribuição Pantropical dessas plantas (Van der Stocken, Carroll, et al., 2019). Entretanto, a riqueza de espécies não é homogênea ao longo de toda essa extensão. A região biogeográfica do Oceano Índico e Oeste do Oceano Pacífico (*Indo-West Pacific region*, IWP) apresenta uma maior diversidade de espécies comparada à da região biogeográfica do Atlântico e Leste do Pacífico (Figura 1) (*Atlantic-East Pacific region*, AEP), com cerca de 54 e 17 espécies, respectivamente (Duke, 2017; Tomlinson, 2016). Essa "anomalia" na riqueza de espécies tem sido tema de discussão na determinação da origem dos mangues (Ellison et al., 1999; He et al., 2022; Ricklefs et al., 2006). Hoje, a teoria mais aceita é a de que os mangues surgiram no fim do Cretáceo, no mar de Thetys, há cerca de 60-90 milhões de anos e algumas linhagens, como *Avicennia*, *Nypa, Ceriops, Pelliciera, Rhizophora* e *Acrostichum*, se distribuíram por amplas áreas. Após seu fechamento, por vicariância, foram isoladas as linhagens percursoras dos grupos que hoje se encontram nas regiões AEP e IWP (Duke, 2017; Ellison et al., 1999). Posteriormente, na IWP, fatores históricos e geográficos como as flutuações no nível do mar e o recorte do litoral das ilhas do Sudeste Asiático, promovendo um ambiente mais fragmentado, teriam como resultado

a formação e manutenção de uma maior diversidade de espécies (He et al., 2019, 2022; Ricklefs et al., 2006).

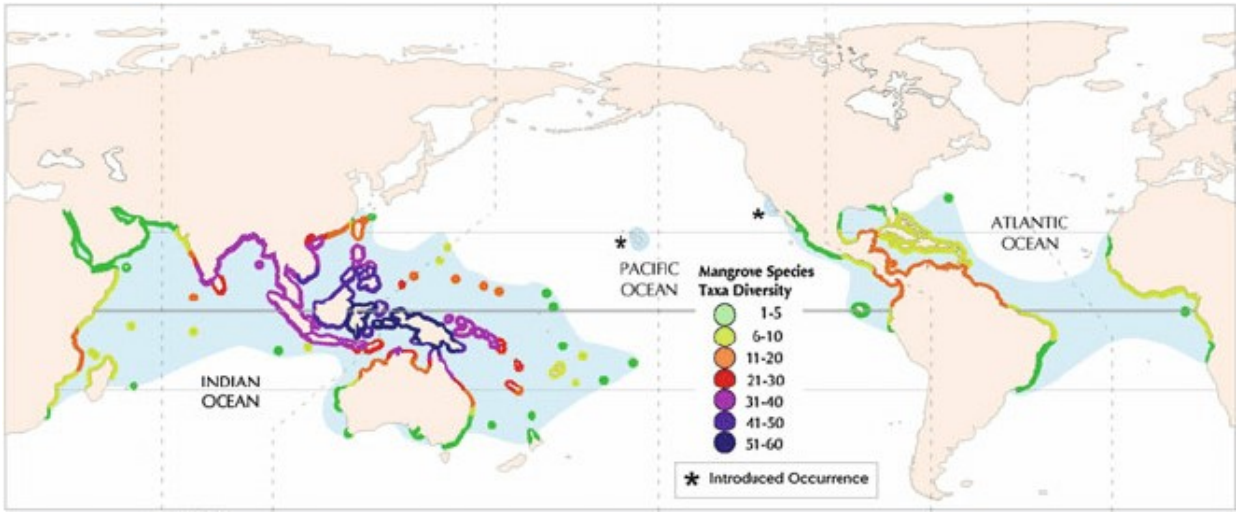

Figura 1. Riqueza de espécies de mangue ao redor do mundo. Adaptado de Duke (2017).

Além da maior diversidade, essas duas regiões biogeográficas apresentam linhagens que evoluem de modo independente. Embora três gêneros, *Avicennia*, *Rhizophora* e *Acrostichum*, estejam presentes tanto em AEP quanto em IWP, as linhagens são reciprocamente monofiléticas em cada região (Duke, 2017). Estudos recentes revelaram a importância da dispersão de longa distância (*Long Distance Dispersal,* LDD) no contato secundário entre AEP e IWP, como observado para *R. samoensis* (Lo et al., 2014; Mori et al., 2021; Takayama et al., 2021; Van der Stocken, Carroll, et al., 2019). Essa espécie do Sul do Pacífico (pertencente à região do IWP) é geneticamente indistinguível das populações de *R. mangle* da costa Leste do Oceano Pacífico (Lo et al., 2014; Mori et al., 2021; Takayama et al., 2021).

Apesar das diferenças biogeográficas, as florestas de mangue em geral são funcionalmente similares e prestam serviços ecossistêmicos parecidos independentemente da localização na IWP ou AEP. Manguezais atuam como berçário para espécies de peixes e invertebrados (Henkens et al., 2022; Lefcheck et al., 2019) e são importantes para o sustento e manutenção de populações humanas com o fornecimento de alimento e madeira, mitigação de eventos climáticos extremos e sequestro de carbono (Alemu I et al., 2021; Howard et al., 2017).

Apesar dos diversos serviços ecossistêmicos prestados, os manguezais sofrem intensa degradação e fragmentação (Bryan-Brown et al., 2020; Kanniah et al., 2021), apesar da diminuição das taxas de perdas de cobertura com esse ecossistema recentemente (Friess et al., 2019). As mudanças climáticas também ameaçam sua integridade e distribuição, com estudos recentes destacando a expansão dos manguezais em direção aos polos, seguindo o aumento da temperatura média, e retração em regiões onde os níveis de chuva vem diminuindo (Cavanaugh et al., 2014; Osland et al., 2017), o que torna os estudos de distribuição de espécies de mangue cruciais para esforços de conservação. Essas alterações em distribuição para espécies sésseis, como mangues, são moduladas pela dispersão por propágulos (Tomlinson, 2016; Van der Stocken, Wee, et al., 2019).

O gênero Rhizophora

O gênero *Rhizophora* é um dos principais gêneros de mangue, dominando as paisagens nas regiões do IWP e do AEP (Tomlinson, 2016). Evidências moleculares e fósseis indicam que a linhagem se divergiu há cerca de 38,6 milhões de anos (Xu et al., 2017), com posterior diversificação entre 1,2 e 6,4 milhões de anos (He et al., 2019). No AEP, o gênero é representado por duas espécies descritas: *R. mangle*, com ampla distribuição pelas costas Leste e Oeste do continente Americano até as ilhas do Pacífico Sul, onde é tradicionalmente identificada como *R. samoensis* (Tomlinson, 2016), e *R. racemosa*, restrita à costa oeste da África, Norte da América do Sul e a uma pequena região da costa do Pacífico na América Central, ocorrendo de forma descontínua (Lo et al., 2014; Menezes et al., 2008). Nas regiões onde *R. mangle* e *R. racemosa* estão em simpatria, há a ocorrência de um híbrido putativo, *R.* × *harrisonii* (Cerón-Souza et al., 2010, 2014; Cornejo, 2013; Mori et al., 2021; Tomlinson, 2016). Além disso, populações das costas do Atlântico e do Pacífico nas Américas parecem representar linhagens distintas entre si, formadas após o surgimento do istmo do Panamá, de forma que as populações de *R. mangle* da costa do Atlântico são mais proximamente relacionadas com as populações de *R. racemosa* do Atlântico do que com as populações de *R. mangle* encontradas na costa do Pacífico (Mori et al., 2021; Takayama et al., 2013, 2021).

No IWP também são observadas espécies híbridas de *Rhizophora*; *R.* × *lamarckii*, híbrida de *R. apiculata* e *R. stylosa* (Chen, 1996), e *R.* × *sellala*, híbrida de *R. samoensis* e *R.*

stylosa (Takayama et al., 2021; Tomlinson, 2016). *R.* × *sellala* representa, portanto, um contato secundário entre as linhagens do IWP e do AEP, uma vez que *R. samoensis* deve ter alcançado o Sul do Pacífico após um ou mais eventos de LDD a partir da costa Oeste do continente Americano, unindo as duas linhagens após milhões de anos de separação (Takayama et al., 2021). A complexa história evolutiva do gênero, com eventos de dispersão transoceânicos e presença cosmopolita, torna-o um bom modelo para estudar a história da distribuição e conectividade de mangues como um todo.

Estudos de distribuição e conectividade de mangues

Mangues possuem uma grande capacidade de dispersão através de seus propágulos com alta flutuabilidade e longevidade, além de resistir por longos períodos à água salgada (Clarke et al., 2001; Rabinowitz, 1978). Essas propriedades permitem que essas unidades dispersoras viagem por longas trajetórias, uma vez que as correntes oceânicas são vetores eficientes de transporte (Nathan et al., 2008; Van der Stocken, Carroll, et al., 2019; Van der Stocken, Wee, et al., 2019). O potencial deslocamento ao longo de milhares de quilômetros traz desafios para o estudo da dispersão de mangues.

O processo de dispersão em mangues se inicia com a soltura do propágulo da planta mãe. Nessa fase, a fenologia e a fecundidade influenciam diretamente a quantidade de propágulos que potencialmente dispersarão (Van der Stocken, Wee, et al., 2019). Posteriormente, caso o propágulo não seja predado ou perdido sua viabilidade, ocorre a fase de transporte, no qual tanto as características do propágulo (forma, densidade, tamanho, flutuabilidade, por exemplo) quanto do meio (e.g., temperatura, salinidade, densidade, força e direção da água e do vento) influenciam no destino da unidade dispersora (Van der Stocken, Carroll, et al., 2019; Van der Stocken, Wee, et al., 2019). Finalmente, durante a imigração, o propágulo que chega a um determinado local e se estabelece, chegando à fase reprodutiva, finaliza o ciclo de dispersão (Van der Stocken, Wee, et al., 2019). Uma vez que fatores físico-químicos e bióticos influenciam a dispersão em diferentes escalas de tempo e espaço, existem diversos métodos que capturam apenas parte desse processo. Uma abordagem flexível em termos de escala espacial (paisagem *vs*. biogeográfica) e temporal (ecológica *vs*. evolutiva) é o uso de evidências genéticas, as quais revelam a dispersão efetiva e a conectividade resultante.

Na região do IWP, ao longo da Península da Malásia, as correntes oceânicas são cruciais para a estruturação genética de *R. mucronata* (Wee et al., 2014); neste caso, a península não atuaria como barreira geográfica, e as populações se encontrariam estruturadas entre o mar de Adaman e o estreito de Malacca, separados por diferentes correntes oceânicas. Outras espécies de mangue com menor potencial de dispersão (como com tamanho reduzido de propágulos e menor longevidade e flutuabilidade), entretanto, apresentaram maiores limitações ao fluxo gênico ao longo desta península, sugerindo que ela atue como um filtro à dispersão efetiva de mangues, e não como uma barreira (Wee et al., 2020). A degradação ambiental também pode influenciar a conectividade; nos manguezais de Sundarban, em Bangladesh, as populações de *Avicennia officinalis* encontram-se isoladas geneticamente em áreas de florestas degradadas, enquanto é observada grande conectividade em regiões de mata nativa (Hasan et al., 2018). Em conjunto, esses trabalhos demonstram a influência de características bióticas (propriedades morfológicas e funcionais dos propágulos) e abióticas (degradação ambiental, correntes oceânicas e massas continentais) no processo de dispersão em diversas escalas.

Já na AEP, é destacada a importância do continente americano como barreira à dispersão entre as populações das costas do Pacífico e do Atlântico, o fluxo gênico entre as populações da costa oeste africana e da costa leste das Américas, e entre as populações da costa oeste das Américas e ilhas do Pacífico Sul. Esses padrões foram observados utilizando evidências obtidas a partir de DNA cloroplastidial (cpDNA) e marcadores microssatélites (Takayama et al., 2013, 2021) e, posteriormente, polimorfismos de base única (*single nucleotide polyporphisms*, SNPs) (Mori et al., 2021). Ainda na região do AEP, foi sugerida a importância das correntes oceânicas e da dispersão de pólen pelo vento na conectividade de *R. mangle* e *Laguncularia racemosa* a partir de dados de SNPs e cpDNA no Caribe (Hodel et al., 2018), com destaque para a importância da dispersão por pólen em *R. mangle* nessa região. Já na costa do Camarões, Ngeve e colaboradores (2021) investigaram propágulos de *R. racemosa* encontrados em uma praia livre de manguezais na costa camaronesa, estimando seu relacionamento com as populações de mangue mais próximas. Entretanto, os propágulos encontrados estavam isolados geneticamente dessas populações, indicando que foram provenientes de populações mais distantes (>300km), além das fronteiras do Camarões, evidenciando a importância de estudos de dispersão de escalas continentais e políticas de conservação intergovernamentais (Ngeve et al. 2021).

No Brasil, diversos estudos (Cruz et al. 2019, 2020; Francisco et al. 2018; Mori et al. 2015; Pil et al. 2011; da Silva et al. 2021) realizados com marcadores moleculares evidenciaram uma divisão entre populações de árvores de mangue ao Norte e ao Sul da extremidade nordeste da América do Sul (*northeastern extremity of South America*, NEESA). Esse padrão foi observado para *R. mangle* (Francisco et al., 2018; Pil et al., 2011), *A. schaueriana* e *A. germinans* (Cruz et al. 2019, 2020; Mori et al. 2015; da Silva et al. 2021), mas não para *L. racemosa* (Sereneski et al., 2021). Em conjunto, esses resultados sugerem que um fator importante, mas não absoluto, para a dispersão de propágulos de mangue seja o padrão de correntes oceânicas que se bifurcam na NEESA (Lumpkin & Johnson 2013), influenciando o trânsito de propágulos entre populações e afetando diretamente o fluxo gênico. A corrente Sul Equatorial encontra a costa brasileira na NEESA e se divide na corrente Norte Brasileira, mais veloz, em direção ao Caribe, e na corrente Brasileira, mais lenta, em direção ao Sul da América do Sul (Lumpkin & Johnson, 2013), isolando as duas regiões. Para o gênero *Avicennia,* a adaptação à disponibilidade de água doce parece ser outro fator preponderante que molda a diversidade genética e fenotípica das populações, o que pode influenciar no recrutamento de novos indivíduos provenientes de eventos de LDD (Cruz et al., 2019, 2020). Isso demonstra que, também para a AEP, como o esperado, diversos fatores bióticos e abióticos podem influenciar a dispersão efetiva de populações de mangue.

Apesar da relativa extensa literatura sobre a dispersão de mangues utilizando marcadores moleculares, são raros os estudos que utilizam mais do que uma fonte de informação, e os trabalhos existentes lidam com escalas de poucas centenas de quilômetros. Por meio de marcadores microssatélite e simulação oceanográfica do trânsito de propágulos ao longo da costa, demonstrou-se que a distribuição atual de *R. racemosa* corresponde melhor a características atuais das correntes locais do que a eventos geológicos ancestrais (Ngeve et al., 2016). De modo complementar, utilizando estes mesmos marcadores moleculares associados à uma estratégia de captura e recaptura de propágulos, observou-se que o transporte de propágulos no rio Wouri é bidirecional, sugerindo que a maré e o vento têm grande importância na dispersão em pequena escala (Ngeve et al., 2017). Em conjunto, esses trabalhos evidenciam como a associação de estratégias de estudo aumentam a capacidade de se identificar fatores que poderiam passar despercebidos se as metodologias fossem utilizadas isoladamente. Cada vez mais, não surpreendentemente, estratégias semelhantes vêm sendo adotadas no estudo de outros

grupos de organismos (Bertola et al., 2020; Jahnke & Jonsson, 2022; Liu et al., 2021; Nikolic et al., 2020). No Sudeste do Atlântico, existe uma grande sub-representação deste tipo de estudo, em especial com espécies de Angiospermas (Jahnke & Jonsson, 2022).

Objetivos

A hipótese da estruturação das populações de mangue ao Norte e ao Sul da NESSA como consequência do padrão das correntes oceânicas na região não foi formalmente testada. Nesse presente trabalho, **nosso objetivo foi avaliar o papel das correntes oceânicas na dispersão e conectividade de *R. mangle* ao longo de toda a costa brasileira**. Para isso, utilizamos simulação da dispersão de propágulos (para estimar o trânsito potencial de unidades dispersoras) e estimativas de taxas de migração a partir de marcadores moleculares (para estimar a migração efetiva, onde ocorre o estabelecimento). Utilizamos SNPs obtidos pelo sequenciamento de fragmentos de DNA associado a sítios de restrição (*Restriction site associated DNA sequencing*, RADseq) para acessar a estrutura genética das populações e estimar as taxas de migração recente e ancestral. Simulamos a dispersão de propágulos por dois modelos distintos de circulação das correntes oceânicas para estimar o transporte de partículas. Por fim, aplicamos testes de Mantel e análises de redundância para testar nossas hipóteses de distribuição de *R. mangle* na costa brasileira.

Esta dissertação está apresentada em um capítulo único, em formato de artigo científico. A coleta dos dados e a montagem da biblioteca de RADseq foram realizadas anteriormente ao início desse projeto pelo nosso grupo de pesquisa. As etapas de detecção de SNPs neutros e a atribuição de indivíduos a populações foram realizadas em conjunto com a aluna de graduação Maria Constance de Almeida, sob coorientação de André G. Madeira e orientação de Gustavo M. Mori. Esse projeto de mestrado resulta do esforço científico de uma equipe de pesquisadores e pesquisadoras, que trabalharam durante as etapas de coleta de material vegetal, extração, purificação e preparação de DNA, além da construção e sequenciamento de bibliotecas genômicas.

Referências

Alemu I, J. B., Richards, D. R., Gaw, L. Y.-F., Masoudi, M., Nathan, Y., & Friess, D. A. (2021). Identifying spatial patterns and interactions among multiple ecosystem services in an urban mangrove landscape.

Ecological Indicators, *121*, 107042. https://doi.org/10.1016/j.ecolind.2020.107042

Bertola, L. D., Boehm, J. T., Putman, N. F., Xue, A. T., Robinson, J. D., Harris, S., Baldwin, C. C., Overcast, I., & Hickerson, M. J. (2020). Asymmetrical gene flow in five co-distributed syngnathids explained by ocean currents and rafting propensity. *Proceedings of the Royal Society B: Biological Sciences*, *287*(1926). https://doi.org/10.1098/rspb.2020.0657

Bryan-Brown, D. N., Connolly, R. M., Richards, D. R., Adame, F., Friess, D. A., & Brown, C. J. (2020). Global trends in mangrove forest fragmentation. *Scientific Reports*, *10*(1), 7117. https://doi.org/10.1038/s41598-020-63880-1

Cavanaugh, K. C., Kellner, J. R., Forde, A. J., Gruner, D. S., Parker, J. D., Rodriguez, W., & Feller, I. C. (2014). Poleward expansion of mangroves is a threshold response to decreased frequency of extreme cold events. *Proceedings of the National Academy of Sciences*, *111*(2), 723–727. https://doi.org/10.1073/pnas.1315800111

Cerón-Souza, I., Rivera-Ocasio, E., Medina, E., Jiménez, J. A., McMillan, W. O., & Bermingham, E. (2010). Hybridization and introgression in new world red mangroves, *Rhizophora* (Rhizophoraceae). *American Journal of Botany*, *97*(6), 945–957. https://doi.org/10.3732/ajb.0900172

Cerón-Souza, I., Turner, B. L., Winter, K., Medina, E., Bermingham, E., & Feliner, G. N. (2014). Reproductive phenology and physiological traits in the red mangrove hybrid complex (*Rhizophora mangle* and *R. racemosa*) across a natural gradient of nutrients and salinity. *Plant Ecology*, *215*(5), 481–493. https://doi.org/10.1007/s11258-014-0315-1

Chen, H. T. (1996). A note on the discovery of *Rhizophora* X *lamarckii* in peninsular Malaysia. *Journal of Tropical Forest Science*, *9*(1), 128–130. http://agris.upm.edu.my:8080/dspace/handle/0/14051

Clarke, P. J., Kerrigan, R. A., & Westphal, C. J. (2001). Dispersal potential and early growth in 14 tropical mangroves: do early life history traits correlate with patterns of adult distribution? *Journal of Ecology*, *89*(4), 648–659. https://doi.org/10.1046/j.0022-0477.2001.00584.x

Cornejo, X. (2013). Lectotypification and a New Status for *Rhizophora* X *Harrisonii* (Rhizophoraceae), a Natural Hybrid Between *R. Mangle* and *R. Racemosa*. *Harvard Papers in Botany*, *18*(1), 37. https://doi.org/10.3100/025.018.0106

Cruz, M. V., Mori, G. M., Oh, D. H., Dassanayake, M., Zucchi, M. I., Oliveira, R. S., & Souza, A. P. de. (2020). Molecular responses to freshwater limitation in the mangrove tree *Avicennia germinans* (Acanthaceae). *Molecular Ecology*, *29*(2), 344–362. https://doi.org/10.1111/mec.15330

Cruz, M. V., Mori, G. M., Signori-Müller, C., da Silva, C. C., Oh, D.-H., Dassanayake, M., Zucchi, M. I., Oliveira, R. S., & de Souza, A. P. (2019). Local adaptation of a dominant coastal tree to freshwater availability and solar radiation suggested by genomic and ecophysiological approaches. *Scientific Reports*, *9*(1), 19936. https://doi.org/10.1038/s41598-019-56469-w

da Silva, M. F., Cruz, M. V., de Deus Vidal Júnior, J., Mori, G. M., Zucchi, M. I., & de Souza, A. P. (2020). Geographic and environmental contributions to genomic divergence in mangrove forests. *BioRxiv*. https://doi.org/10.1101/2020.01.08.889717

Duke, N. C. (2017). Mangrove Ecosystems: A Global Biogeographic Perspective. In V. H. Rivera-Monroy, S. Y. Lee, E. Kristensen, & R. R. Twilley (Eds.), *Mangrove Ecosystems: A Global Biogeographic Perspective: Structure, Function, and Services* (Issue January, pp. 1–399). Springer International Publishing. https://doi.org/10.1007/978-3-319-62206-4

Ellison, A. M., Farnsworth, E. J., & Merkt, R. E. (1999). Origins of mangrove ecosystems and the mangrove biodiversity anomaly. *Global Ecology and Biogeography*, *8*(2), 95–115. https://doi.org/10.1046/j.1466-822X.1999.00126.x

Francisco, P. M., Mori, G. M., Alves, F. M., Tambarussi, E. V., & de Souza, A. P. (2018). Population genetic structure, introgression, and hybridization in the genus *Rhizophora* along the Brazilian coast. *Ecology and Evolution*, *8*(6), 3491–3504. https://doi.org/10.1002/ece3.3900

Friess, D. A., Rogers, K., Lovelock, C. E., Krauss, K. W., Hamilton, S. E., Lee, S. Y., Lucas, R., Primavera, J., Rajkaran, A., & Shi, S. (2019). The State of the World's Mangrove Forests: Past, Present, and Future. *Annual Review of Environment and Resources*, *44*(1), 89–115. https://doi.org/10.1146/annurev-environ-101718-033302

Hasan, S., Triest, L., Afrose, S., & De Ryck, D. J. R. (2018). Migrant pool model of dispersal explains strong connectivity of Avicennia officinalis within Sundarban mangrove areas: Effect of fragmentation and replantation. *Estuarine, Coastal and Shelf Science*, *214*(June), 38–47. https://doi.org/10.1016/j.ecss.2018.09.007

He, Z., Feng, X., Chen, Q., Li, L., Li, S., Han, K., Guo, Z., Wang, J., Liu, M., Shi, C., Xu, S., Shao, S., Liu, X., Mao, X., Xie, W., Wang, X., Zhang, R., Li, G., Wu, W., … Shi, S. (2022). Evolution of coastal forests based on a full set of mangrove genomes. *Nature Ecology & Evolution*, *6*(6), 738–749. https://doi.org/10.1038/s41559-022-01744-9

He, Z., Li, X., Yang, M., Wang, X., Zhong, C., Duke, N. C., Wu, C.-I., & Shi, S. (2019). Speciation with gene flow via cycles of isolation and migration: insights from multiple mangrove taxa. *National Science Review*, *6*(2), 275–288. https://doi.org/10.1093/nsr/nwy078

Henkens, J., Dittmann, S., & Baring, R. (2022). Nursery function of mangrove creeks in temperate climates for estuarine fish. *Transactions of the Royal Society of South Australia*, 1–21. https://doi.org/10.1080/03721426.2022.2035200

Hodel, R. G. J., Knowles, L. L., McDaniel, S. F., Payton, A. C., Dunaway, J. F., Soltis, P. S., & Soltis, D. E. (2018). Terrestrial species adapted to sea dispersal: Differences in propagule dispersal of two Caribbean mangroves. *Molecular Ecology*, *27*(22), 4612–4626. https://doi.org/10.1111/mec.14894

Howard, J., Sutton-Grier, A., Herr, D., Kleypas, J., Landis, E., Mcleod, E., Pidgeon, E., & Simpson, S. (2017). Clarifying the role of coastal and marine systems in climate mitigation. *Frontiers in Ecology and the Environment*, *15*(1), 42–50. https://doi.org/10.1002/fee.1451

Jahnke, M., & Jonsson, P. R. (2022). Biophysical models of dispersal contribute to seascape genetic analyses. *Philosophical Transactions of the Royal Society B: Biological Sciences*, *377*(1846). https://doi.org/10.1098/rstb.2021.0024

Kanniah, K. D., Kang, C. S., Sharma, S., & Amir, A. A. (2021). Remote Sensing to Study Mangrove Fragmentation and Its Impacts on Leaf Area Index and Gross Primary Productivity in the South of Peninsular Malaysia. *Remote Sensing*, *13*(8), 1427. https://doi.org/10.3390/rs13081427

Kathiresan, K., & Bingham, B. L. (2001). *Biology of mangroves and mangrove Ecosystems* (pp. 81–251). https://doi.org/10.1016/S0065-2881(01)40003-4

Lefcheck, J. S., Hughes, B. B., Johnson, A. J., Pfirrmann, B. W., Rasher, D. B., Smyth, A. R., Williams, B. L., Beck, M. W., & Orth, R. J. (2019). Are coastal habitats important nurseries? A meta-analysis. *Conservation Letters*, e12645. https://doi.org/10.1111/conl.12645

Liu, J., Lindstrom, A. J., Chen, Y., Nathan, R., & Gong, X. (2021). Congruence between ocean-dispersal modelling and phylogeography explains recent evolutionary history of *Cycas* species with buoyant seeds. *New Phytologist*, *232*(4), 1863–1875. https://doi.org/10.1111/nph.17663

Lo, E. Y. Y., Duke, N. C., & Sun, M. (2014). Phylogeographic pattern of *Rhizophora* (Rhizophoraceae) reveals the importance of both vicariance and long-distance oceanic dispersal to modern mangrove distribution. *BMC Evolutionary Biology*, *14*(1), 83. https://doi.org/10.1186/1471-2148-14-83

Lumpkin, R., & Johnson, G. C. (2013). Global ocean surface velocities from drifters: Mean, variance, El Niño-Southern Oscillation response, and seasonal cycle. *Journal of Geophysical Research: Oceans*, *118*(6), 2992–3006. https://doi.org/10.1002/jgrc.20210

Menezes, M. P. M. de, Berger, U., & Mehlig, U. (2008). Mangrove vegetation in Amazonia: a review of studies from the coast of Pará and Maranhão States, north Brazil. *Acta Amazonica*, *38*(3), 403–420. https://doi.org/10.1590/S0044-59672008000300004

Mori, G. M., Madeira, A. G., Cruz, M. V., Tsuda, Y., Takayama, K., Matsuki, Y., Suyama, Y., Iwasaki, T., de Souza, A. P., Zucchi, M. I., & Kajita, T. (2021). Testing species hypotheses in the mangrove genus *Rhizophora* from the Western hemisphere and South Pacific islands. *Estuarine, Coastal and Shelf Science*, *248*(June 2020). https://doi.org/10.1016/j.ecss.2020.106948

Mori, G. M., Zucchi, M. I., & Souza, A. P. (2015). Multiple-geographic-scale genetic structure of two mangrove tree species: The roles of mating system, hybridization, limited dispersal and extrinsic factors. *PLoS ONE*, *10*(2), 1–23. https://doi.org/10.1371/journal.pone.0118710

Nathan, R., Schurr, F. M., Spiegel, O., Steinitz, O., Trakhtenbrot, A., & Tsoar, A. (2008). Mechanisms of long-distance seed dispersal. *Trends in Ecology and Evolution*, *23*(11), 638–647. https://doi.org/10.1016/j.tree.2008.08.003

Ngeve, M. N., Koedam, N., & Triest, L. (2021). Genotypes of *Rhizophora* Propagules From a Non-mangrove Beach Provide Evidence of Recent Long-Distance Dispersal. *Frontiers in Conservation Science*, *2*. https://doi.org/10.3389/fcosc.2021.746461

Ngeve, M. N., Van der Stocken, T., Sierens, T., Koedam, N., & Triest, L. (2017). Bidirectional gene flow on a mangrove river landscape and between-catchment dispersal of *Rhizophora racemosa* (Rhizophoraceae). *Hydrobiologia*, *790*(1), 93–108. https://doi.org/10.1007/s10750-016-3021-2

Ngeve, M. N., Vanderstocken, T., Menemenlis, D., Koedam, N., & Triest, L. (2016). Contrasting effects of historical sea level rise and contemporary ocean currents on regional gene flow of *Rhizophora racemosa* in eastern atlantic mangroves. *PLoS ONE*, *11*(3), 1–24. https://doi.org/10.1371/journal.pone.0150950

Nikolic, N., Montes, I., Lalire, M., Puech, A., Bodin, N., Arnaud-Haond, S., Kerwath, S., Corse, E., Gaspar, P., Hollanda, S., Bourjea, J., West, W., & Bonhommeau, S. (2020). Connectivity and population structure of albacore tuna across southeast Atlantic and southwest Indian Oceans inferred from multidisciplinary methodology. *Scientific Reports*, *10*(1), 15657. https://doi.org/10.1038/s41598-020-72369-w

Osland, M. J., Feher, L. C., Griffith, K. T., Cavanaugh, K. C., Enwright, N. M., Day, R. H., Stagg, C. L., Krauss, K. W., Howard, R. J., Grace, J. B., & Rogers, K. (2017). Climatic controls on the global distribution, abundance, and species richness of mangrove forests. *Ecological Monographs*, *87*(2), 341–359. https://doi.org/10.1002/ecm.1248

Pil, M. W. W., Boeger, M. R. T. T. R. T., Muschner, V. C. C., Pie, M. R. R., Ostrensky, A., & Boeger, W. A. A. (2011). Postglacial north-south expansion of populations of *Rhizophora mangle* (Rhizophoraceae) along the Brazilian coast revealed by microsatellite analysis. *American Journal of Botany*, *98*(6), 1031–1039. https://doi.org/10.3732/ajb.1000392

Rabinowitz, D. (1978). Dispersal Properties of Mangrove Propagules. *Biotropica*, *10*(1), 47–57.

Ricklefs, R. E., Schwarzbach, A. E., & Renner, S. S. (2006). Rate of Lineage Origin Explains the Diversity Anomaly in the World's Mangrove Vegetation. *The American Naturalist*, *168*(6), 805–810. https://doi.org/10.1086/508711

Takayama, K., Tamura, M., Tateishi, Y., Webb, E. L., & Kajita, T. (2013). Strong genetic structure over the American continents and transoceanic dispersal in the mangrove genus *Rhizophora* (Rhizophoraceae) revealed by broad- scale nuclear and chloroplast DNA analysis. *American Journal of Botany*, *100*(6), 1191–1201. https://doi.org/10.3732/ajb.1200567

Takayama, K., Tateishi, Y., & Kajita, T. (2021). Global phylogeography of a pantropical mangrove genus *Rhizophora*. *Scientific Reports*, *11*(1), 7228. https://doi.org/10.1038/s41598-021-85844-9

Tomlinson, P. B. (2016). *The Botany of Mangroves*. Cambridge University Press. https://doi.org/10.1017/CBO9781139946575

Van der Stocken, T., Carroll, D., Menemenlis, D., Simard, M., & Koedam, N. (2019). Global-scale dispersal and connectivity in mangroves. *Proceedings of the National Academy of Sciences*, *116*(3), 915–922. https://doi.org/10.1073/pnas.1812470116

Van der Stocken, T., Wee, A. K. S., De Ryck, D. J. R., Vanschoenwinkel, B., Friess, D. A., Dahdouh-Guebas, F., Simard, M., Koedam, N., & Webb, E. L. (2019). A general framework for propagule dispersal in mangroves. *Biological Reviews*, *94*(4), 1547–1575. https://doi.org/10.1111/brv.12514

Wee, A. K. S., Noreen, A. M. E., Ono, J., Takayama, K., Kumar, P. P., Tan, H. T. W., Saleh, M. N., Kajita, T., & Webb, E. L. (2020). Genetic structures across a biogeographical barrier reflect dispersal potential of four Southeast Asian mangrove plant species. *Journal of Biogeography*, *47*(6), 1258–1271. https://doi.org/10.1111/jbi.13813

Wee, A. K. S., Takayama, K., Asakawa, T., Thompson, B., Onrizal, Sungkaew, S., Tung, N. X., Nazre, M., Soe, K. K., Tan, H. T. W., Watano, Y., Baba, S., Kajita, T., & Webb, E. L. (2014). Oceanic currents, not land masses, maintain the genetic structure of the mangrove *Rhizophora mucronata* Lam. (Rhizophoraceae) in Southeast Asia. *Journal of Biogeography*, *41*(5), 954–964. https://doi.org/10.1111/jbi.12263

Xu, S., He, Z., Zhang, Z., Guo, Z., Guo, W., Lyu, H., Li, J., Yang, M., Du, Z., Huang, Y., Zhou, R., Zhong, C., Boufford, D. E., Lerdau, M., Wu, C.-I. I., Duke, N. C., Shi, S., Lee, S. Y., Li, X., … Baereleo, R. T. (2017). The origin, diversification and adaptation of a major mangrove clade (Rhizophoreae) revealed by whole-genome sequencing. *National Science Review*, *4*(5), 721–734. https://doi.org/10.1093/nsr/nwx065

Capítulo I.

The role of oceanic currents in the dispersal and connectivity of the mangrove *Rhizophora mangle* on the Southwest Atlantic region

Short title: Oceanic currents and dispersal of a mangrove.

Authors: André Guilherme Madeira[1✉], Yoshiaki Tsuda[2], Yukio Nagano[3], Takaya Iwasaki[4], Maria Imaculada Zucchi[5], Tadashi Kajita[6], Gustavo Maruyama Mori[1]

✉Correspondence: André Guilherme Madeira <madeira.ag@gmail.com>

[1] São Paulo State University (Unesp), Institute of Biosciences, São Vicente, Brazil

[2] Sugadaira Research Station, Mountain Science Center, University of Tsukuba, Nagano, Japan

[3] Analytical Research Center for Experimental Sciences, Saga University, Saga, Japan

[4] Faculty of Science, Ochanomizu University, Tokyo, Japan

[5] Agência Paulista de Tecnologia dos Agronegócios, Piracicaba, Brazil

[6] Iriomote Station, Tropical Biosphere Research Center, University of the Ryukyus, Japan

O manuscrito foi redigido de acordo com a formatação exigida para publicação pela revista Molecular Ecology Resources

Abstract

Dispersal is a crucial mechanism to living beings, allowing them to reach new resources such that populations and species can explore new environment conditions. However, describing dispersal mechanisms of widespread species can be costly or even impracticable, which is the case for mangrove trees. The influence of ocean currents on the mangroves' propagules' movement has been increasingly evident; however, few studies mechanistically relate the patterns of population distribution with the dispersal by oceanic currents under an integrated framework. Here, we evaluate the role of oceanic currents on dispersal and connectivity of *Rhizophora mangle* along the Southwest Atlantic basin. We inferred population genetic structure and migration rates based on single nucleotide polymorphisms, simulated the displacement of propagules along the Southwest Atlantic coast and tested our hypotheses with Mantel tests and redundancy analysis. We observed a two populations structure, north and south, which is corroborated by other studies with *Rhizophora* and other coastal plants. The inferred recent migration rates do not indicate gene flow between the sampled sites. Conversely, long-term migration rates were low across groups and contrasting dispersal patterns within each one, which is consistent with long-distance dispersal events. Our hypothesis tests suggests that both isolation by distance and isolation by oceanography (derived from the oceanic currents) can explain the neutral genetic variation of *R. mangle* in the region. Our findings expand the current knowledge of mangrove connectivity and highlight how the association of molecular methods with oceanographic simulations improve the interpretation power of the dispersal process, which has ecological and evolutionary implications.

Keywords: Rhizophoraceae, RADseq, LDD, seascape genetics, migration rates.

Introduction

Dispersal is the movement of organisms or units – like seeds and fruits – from their place of origin to a new home range. It is a fundamental process for a species, as it influences its distribution, its resilience to environmental changes (Travis et al. 2013) and establishes connectivity between spatially structured populations (Lowe et al. 2017). The dispersal process can be divided into three stages: (a) emigration, which is the departure of the dispersing individual or unit, (b) transit through the environmental matrix, and (c) immigration, which is the arrival and establishment in the new area of life (Cayuela et al. 2018). Given its biological importance and implications, the study of dispersal mechanisms and their consequences is of great scientific importance and has practical applications, as in the development of management plans and conservation strategies (Driscoll et al. 2014).

To assess effective dispersal, it is necessary to combine strategies to evaluate establishment, assessing the individuals that contribute to the gene pool, and displacement, monitoring or simulating the process of immigration. Establishment can be inferred at multiple time scales, from recent events through kinship tests and parentage assignment, to longer term evaluations, using, for example, the fixation index (F_{ST}) or demographic inferences based on genetic approaches (Nathan et al. 2003; Cayuela et al. 2018). Displacement can be evaluated by telemetry and capture and recapture methods, for example. Both have been used to study seasonal migration and foraging, but are less suitable to deal with less frequent and more unpredictable movements such as long-distance dispersal (LDD) (Nathan et al. 2003; Shafer et al. 2016; Cayuela et al. 2018). LDD events, on the order of thousands of kilometers, are rare events for most species, but they can have major demographic consequences and therefore should not be underestimated (Nathan 2006).

The study of LDD events is costly and it is often impractical to directly monitor dispersal mechanisms, and it is usually impossible to extrapolate regional ecological data for scales of this magnitude (Bullock and Nathan 2008). LDD is especially important for marine species (Villarino et al. 2018), as oceanic currents play a major role in their displacements (Hays et al. 2016; Hays 2017; Lalire and Gaspar 2019; Bertola et al. 2020). The same is true for coastal plants that disperse via seawater. Recent studies have used particle modeling to simulate the dispersal of, among others, coastal grasses (Smith et al. 2018), nettles (Wu et al. 2018) and mangroves (Van der Stocken et al. 2019a).

Mangroves present adaptations to live between land and sea. Among these adaptations are propagules, which are fruits or seeds that can stay afloat for weeks or months at sea without losing its viability (Tomlinson 2016), thus allowing LDD. The genus *Rhizophora* is one of the main mangrove genera, dominating landscapes in the biogeographic regions of Indo West-Pacific (IWP) and Atlantic East-Pacific (AEP) (Tomlinson, 2016). In the AEP, the genus is represented by two described species: *R. mangle*, with wide distribution along the East and West coasts of the American continent to the islands of the South Pacific, where it is traditionally identified as *R. samoensis* (Tomlinson, 2016), and *R. racemosa*, restricted to the west coast of Africa, northern South America and a small region of the Pacific coast of Central America, occurring discontinuously (Lo et al., 2014; Menezes et al., 2008). In regions where *R. mangle* and *R. racemosa* occur in sympatry, there is the occurrence of a putative hybrid, *R.* × *harrisonii* (Cerón-Souza et al., 2010, 2014; Cornejo, 2013; Mori et al., 2021; Tomlinson , 2016). Furthermore, populations from the Atlantic and Pacific coasts of the Americas seem to represent distinct lineages, formed after the emergence of the Isthmus of Panama, so that the populations of *R. mangle* from the Atlantic coast are more closely related to the populations of *R. racemosa* from the Atlantic than with populations of *R. mangle* found on the Pacific coast (Mori et al., 2021; Takayama et al., 2013, 2021). In the IWP, hybrid species of *Rhizophora* are also observed; *R.* × *lamarckii*, a hybrid of *R. apiculata* and *R. stylosa* (Chen, 1996), and *R.* × *sellala*, a hybrid of *R. samoensis* and *R. stylosa* (Takayama et al., 2021; Tomlinson, 2016). *R.* × *sellala* represents, therefore, a secondary contact between the IWP and AEP lineages, since *R. samoensis* must have reached the South Pacific after one or more LDD events from the west coast of the American continent, uniting the two lineages after millions of years of separation (Takayama et al., 2021). The complex evolutionary history of the genus, with transoceanic dispersal events and cosmopolitan presence, makes it a good model to study the history of mangrove distribution and connectivity as a whole.

Recently, mangrove dispersal, distribution and population genetic structure have received substantial attention. Studies based on genetic variation highlighted that multiple factors play important roles shaping the distribution and connectivity of mangrove species and their populations, like the influence of landscape (Wee et al. 2014, 2020; Canty et al. 2022), human activity (Hasan et al. 2018; Geng et al. 2021), land barriers (Mori et al. 2021; Takayama et al. 2021) and oceanic currents (Hodel et al. 2018; Van der Stocken et al. 2019a; Da Silva et

al. 2021; Ngeve et al. 2021; Sereneski-Lima et al. 2021). Despite the relatively extensive literature on mangrove dispersal using molecular markers, studies using more than one source of information are rare, and existing research deals with scales of a few hundred kilometers. Using the genetic information obtained by microsatellites markers coupled with oceanographic physical simulation it was shown that the distribution of *Rhizophora racemosa* along the coast corresponds better to characteristics of local currents than to ancestral geological events (Ngeve et al. 2016). At a finer scale, capture-recapture methods coupled with the same molecular tools showed that transport of propagules in the Wouri River is bidirectional, suggesting that tide and wind play a major role in the dispersal (Ngeve et al. 2017). Similar studies that integrate different methodologies such as those carried out for the Cameroonian coast are rare, but increasingly common in other groups of organisms (Bertola et al. 2020; Nikolic et al. 2020; Liu et al. 2021; Jahnke and Jonsson 2022).

Here, we evaluate the role of ocean currents in the dispersal and connectivity of *Rhizophora mangle* along the Southwest Atlantic basin. We used single nucleotide polymorphisms (SNPs) to describe population genetic structure and estimate recent and ancient migration rates as proxies of effective dispersal. We combined these findings based on molecular variation with estimates of particles transport via oceanic currents using two biophysical models of particle displacement, one mechanistic and one probabilistic. Finally, we tested our hypothesis for the distribution of *R. mangle* populations using Mantel tests and redundancy analysis, which is expected to provide a mechanistic explanation of the dispersal patterns we observed (Jahnke and Jonsson 2022). We tested the null hypothesis (H_0) that assumes that *R. mangle* trees from the Southwest Atlantic basin constitute a single homogenous population. H_0 predicts that the genetic data will not indicate any population structure with substantial migration among the sampling sites and that the biophysical simulations will show an intense exchange of propagules between them. Alternatively (H_1), dispersal would be limited mostly in the immigration phase. According to this hypothesis, one may expect to observe strong, small-scale population genetic structure with little to no migration among sampling sites and that simulated propagules do not disperse far from their places of origin. In a third hypothesis (H_2), responses to different multiple factors would be key to the connectivity of *R. mangle* populations. The corollary of this hypothesis is that one would observe discrepancies between the pattern of inferred migration and the pattern of displacement of the simulated

propagules. Our last hypothesis (H_3) assumes that ocean currents is the sole major factor in the dispersal and establishment of *R. mangle*. Here, we predict that the pattern of inferred migration and genetic structure mirrors the pattern of transport of simulated propagules.

Materials and Methods

Sampling and RAD-seq library preparation and sequencing

We sampled seventy-eight individuals of *R. mangle* from eleven sites across the Southwest Atlantic coast, ranging from 1º 23' S to 28º 25' S (Table 1, Figure 1a). We are aware of the sampling gap between the localities of Tamandaré (TMD) and Guapimirim (GPM). This gap occurs mainly due to limited manpower and resources. We believe that our high sampling number and high number of molecular markers ensures the robustness of our results despite this sampling gap. We were granted licenses to sample *Rhizophora* plants (Instituto Chico Mendes de Conservação da Biodiversidade – ICMBio - 17130) and assess their genetic variation (Sistema Nacional de Gestão do Patrimônio Genético e do Conhecimento Tradicional Associado – SisGen - A885104). The individuals were identified in the field based on leaf and inflorescence morphology (Cerón-Souza et al. 2010). Despite taxonomic issues regarding the genus *Rhizophora* in the Western hemisphere (Cerón-Souza et al. 2010; Francisco et al. 2018; Mori et al. 2021), in the studied area, plants morphologically identified as *R. mangle* comprise a rather homogenous genetic group (Francisco et al., 2018, Mori et al., 2021). The samples we used in this study were previously analyzed on three independent works using different molecular markers (Takayama et al. 2013; Francisco et al. 2018; Mori et al. 2021). We isolated DNA samples from each individual using a regular cetyltrimethylammonium bromide (CTAB) method (Doyle and Doyle, 1990). We affeered DNA integrity with 1% agarose gel electrophoresis and quantity in Quantus™ Fluorometer with QuantiFluor® dsDNA System (Promega, Madison, WI, EUA). Only samples with high quantities (> 250 ng) of high-quality DNA were used to build three RADseq libraries following the original protocol (Baird et al. 2008) with small changes to allow the use of 250 ng of DNA. Briefly, the samples were digested with the restriction enzyme EcoRI (G^AATTC) (Takara, Japan) and fragments were ligated with the adapters P1 (Ilumina) that contain an amplification site, the Ilumina sequencing site and a specific barcode for posterior reads demultiplexing. The fragments were then sheared,

size-selected and ligated with the adapters P2 (Ilumina) that ensure that only P1-ligated fragments are enriched in the subsequent PCR amplification. We then sequenced the libraries with the HiSeq2000 sequencer (Ilumina) at Macrogen (Seoul, South Korea). The individuals analyzed in this work are a part of a broader scale study, including trees sampled across the Western hemisphere and South Pacific islands (Mori et al. 2021).

Table 1. *Rhizophora mangle* sampling sites along the Southwest Atlantic basin.

Acronym (N)	Sampling site (Municipality-State)	Latitude	Longitude
SAL (5)	Salinópolis-PA	1º 23' 44.88'' S	47º 22' 5.16'' W
PAR (4)	Bragança-PA	1º 10' 34.43'' S	46º 36' 59.4'' W
ALC (9)	Alcântara-MA	3º 35' 25.03'' S	44º 24' 20.62'' W
PNB (7)	Parnaíba-PI	3º 13' 10.16'' S	41º 49' 24.89'' W
PRC (8)	Paracuru-CE	4º 35' 14.32'' S	39º 3' 25.49'' W
TMD (8)	Tamandaré-PE	9º 24' 36.94'' S	35º 3' 52.02'' W
GPM (2)	Guapimirim-RJ	23º 18' 3.96'' S	43º 0' 5.47'' W
UBA (10)	Ubatuba-SP	24º 30' 36'' S	45º 9' 46.8'' W
CNN (7)	Cananéia-SP	25º 6' 10.44'' S	47º 50' 49.92'' W
PPR (10)	Pontal do Paraná-PR	26º 22' 37.56'' S	48º 21' 19.44'' W
FLN (8)	Florianópolis-SC	28º 25' 55.92'' S	48º 31' 8.04'' W

N: number of sampled individuals in each site.

SNP calling, filtering and neutral SNP selection

For SNP calling, we used STACKS 2.4 (Rochette and Catchen 2017) to demultiplex reads, cutadapt 2.2 (Martin 2011) to remove adapters and TIMMOMATIC 0.39 (Bolger et al. 2014) to filter reads by quality (Phred score > 33). Following, with bowtie 2.3.5.1 (Langmead and Salzberg 2012), we aligned reads to the reference genome of *R. apiculata* (NCBI Project PRJEB8423; Xu et al., 2017), used SAMtools 1.9 (Li 2011) to index, list and organize reads

and bcftools 1.9 (Narasimhan et al. 2016) to identify SNPs. Finally, VCFtools v0.1.16 (Danecek et al. 2011) was used to filter out individuals and loci based on their missing data. Different filters with different missing data permissibility were tested to maximize loci and individual retained and minimize the amount of missing data. We filtered out individuals with more than 20% missing data and loci missing from more than 20% individuals and with less than three minor allele count.

As an effort to only analyze neutral markers, we used several approaches to identify signatures of natural selection because methods to test markers neutrality may generate large numbers of false positives (François et al. 2016; Grünwald et al. 2017). We used LOSITAN (Antao et al. 2008), which detects markers at the edge of the F_{ST} distribution curve with the FDIST2 method (Beaumont and Nichols 1996). This method evaluates the expected neutral relationship between F_{ST} and the expected heterozygosity across all loci to identify outlier loci (those that have excessively high or low F_{ST}). Secondly, we used pcadapt 4.1.0 (Luu et al. 2017), which implements a principal component analysis (PCA) to identify whether a marker has a significantly different F_{ST}. By using a PCA to determine the groupings of individuals, pcadapt does not require prior population structure information to identify outliers and can handle admixed individuals better than other strategies (Luu et al. 2017). Lastly, we used a Bayesian approach to identify F_{ST} outliers with Bayescan 2.1 (Foll and Gaggiotti 2008). Bayescan is especially effective at handling small samples, since its Bayesian method incorporate the uncertainty of allele frequencies due to small sample sizes, reducing bias. In all cases, we filtered out the SNPs with false discovery rate (FDR) < 0.1.

In addition to the F_{ST} methods, we used a latent factors mixed models (LFMM) implemented in the packages LEA 3.6.0 and LFMM 1.0 (Frichot et al. 2013), which allow us to associate allelic frequencies and environmental factors to identify putative loci under selection. For this analysis, we also considered an FDR of 0.1. We obtained data regarding temperature, precipitation, water vapor pressure, solar radiation (collected from WordClim2) (Fick and Hijmans 2017), sea-surface salinity and temperature (collected from MARSPEC) (Sbrocco and Barber 2013), tide amplitudes and number and duration of tidal cycles (collected from the Environmental Climate Data Sweden, ECDS) (Obst 2017). For downstream analyses, we utilized only the SNPs with no evidence of natural selection in at least three of these methods.

Population structure and effective migration surfaces

To assign individuals to populations, we used admixture 1.3.0 (Alexander et al. 2009), which implements a genetic model that presumes correlated allelic frequencies and ancestral mixture. We ran admixture for values of K (number of genetic groups) varying from 1 to 11 and compared the cross-validation error of different runs to determine the best values for K. Complementarily, we used adegenet 2.1 (Jombart and Ahmed 2011) to perform a discriminant analysis of principal components (DAPC) to identify populations regardless of genetic models, focusing on describing the differences between the inferred groups and minimizing variation within clusters (Jombart et al. 2010). K, in this case, was chosen by the smallest Bayesian information criterion (BIC) score after an initial PCA. We calculated the Slatkin-linearized pairwise F_{ST} (Weir and Cockerham 1984; Slatkin 1995) between sampling sites and between inferred groups (see Results) using arlequin v3.5.2.2 (Excoffier & Lischer, 2010).

We also described population structure of *R. mangle* across the Southwest Atlantic basin by inferring effective migration surfaces with EEMS v1.0 (Petkova et al. 2015). This method utilizes the isolation by distance model as null hypothesis and returns the deviations of this model in the observed gene flow for georeferenced genetic samples. Using this model-based method, one may estimate a migration parameter *m*, which allows the characterization of genetic divergence between demes. EEMS enables the visualization of population structure in a surface that highlights regions with high gene flow and migration barriers. We assembled the grid considering only in-water demes in the Southwest Atlantic region, and ran five independent runs, with 10^7 Markov chain Monte Carlo steps (MCMC) and 10^6 burn-in, with deme size of 10^3.

Migration inference

To quantify effective connectivity among populations, we used two approaches. The first estimates recent (i.e., contemporary) directional migration rates, over few generations, implemented in BA3-SNPs 1.1 (Mussmann et al. 2019), which is a modification of BayessAss 3 (Wilson and Rannala 2003) to work with large SNPs datasets. BayessAss implements a

Bayesian MCMC method to estimate asymmetric recent migration rates, which are the proportion of each population with migrant ancestry (Wilson and Rannala 2003). We ran 10^8 iterations, with 10^6 burn-in and sampling interval of 100. The mixing parameters for allelic frequency, inbreeding coefficient and migration rate were set as 0.9, 0.05 and 0.1, respectively, adjusted for an acceptance rate between 20% and 40% (Wilson and Rannala 2003).

To complement BA3-SNPs analyses, we estimated ancestral (i.e., long-term) migration rates based on site frequency spectrum (SFS, obtained with arlequin v3.5.2.2) (Excoffier & Lischer, 2010) with fastsimcoal26 (Excoffier et al. 2021). Given a complex demographic model, fastsimcoal26 simulates the neutral genetic diversity of samples and their ancestors trough a coalescent method. Thus, it can be used to test different complex evolutionary scenarios, accounting for population resizes and hybridization, and to infer parameters like divergence time, effective population sizes and migration rates (Excoffier et al. 2021). To reduce computational demand and allow time-consuming simulations, we inferred the ancestral migration rates based on the population genetic structure we observed (see Results): only among the north group sampling sites (SAL, PAR, ALC, PNB and PRC) and among the south group sampling sites (TMD, GPM, UBA, CNN, PPR and FLN). We evaluated three different scenarios for each setting: panmixia, steppingstone and directional migration (Supplementary Information 1, 2 and 3, respectively). In the panmixia scenario, we inferred the ancestral migration rates between all sites in their own region. In the steppingstone scenario, we inferred only the ancestral migration rates between neighboring sites, considering the remaining migration rates as zero. Finally, in the directional migration scenario, we assumed east to west migration rates to be ten times higher than the opposite direction, as the oceanic currents would suggest. In addition to these scenarios, we also estimated the ancestral migration rates between the two groups, north and south. We ran fifty independent runs, with 10^6 iterations each for each model, and selected the best run based on the smallest difference between maximum likelihood and observed likelihood (deltaL). We then compared the scenarios based on the Akaike information criterium (AIC) (Aho et al. 2014) of the best run.

Simulation of propagule displacement

We used two methods to estimate the propagule displacement among sites and, thus, provide an oceanographic context to be tested with the genetic-based results. The first is a probabilistic oceanic transport estimate with Adrift (van Sebille 2014), which combines observational data from seventeen thousand floaters released between 1979 and 2013 to track the movement of floating objects with two-month intervals and 1° resolution. This approach disregards the effects of seasonality or year-specific oceanographic conditions, which makes Adrift an adequate tool for historical biogeography studies (Bertola et al. 2020). We simulated the release of mangrove propagules departing from each of the eleven sampling sites to obtain the cumulative probability of presence of particles in each other localities in a two-year period. This value was then divided by the sum of probabilities in every site to build a relative index of directional transport. This 24-months period is a conservative measure of floating period of *Rhizophora* species (Van der Stocken et al. 2019b).

To complement the oceanic transport estimate analysis, we used a mechanistic propagule displacement approach based on the biophysical model of particles dispersal OceanDrift implemented in OpenDrift v1.9.0 (Dagestad et al. 2018). OpenDrift is a framework for trajectory models that tracks the fate of objects drifting in the ocean based on given current velocity data. We used a 1/3º grided horizontal sea surface current velocity data from OSCAR (Ocean Surface Current Analysis Real-time), which are based on sea surface height, surface vector wind and sea surface temperature data from various satellites and *in situ* instruments (Bonjean and Lagerloef 2002). We simulated the release of a total of 10^6 propagules distributed in equal time intervals from 2010 to 2020 from each sampling site and tracked each particle for at least one year. To avoid having all particles trapped inside a bay, release coordinates for PRC, TMD, GPM, CNN and FLN were slightly shifted to open areas to identify the fate of propagules that reach oceanic currents. We disregarded data from particles that drifted for more than one year and registered the number of particles that beached in a 1º radius around each other sampling site.

Drivers of isolation

We tested the relationship between the ancestral migration rates and the simulated propagule displacement trough oceanic currents using Mantel tests (Mantel 1967) modified to consider asymmetrical matrices (Bergmann and McElroy 2014), with 99999 iterations. We also

compared the migration rates with the Euclidian distance among sites and with the minimum in-water distance, computed with package gdistance v1.3-6 for R (van Etten 2017) with the least-cost distance between sites using land mass as an infinite resistance surface (Assis et al. 2013).

In addition to the Mantel tests, we used redundancy analysis (RDA) to model linear relationships between spatial eigenvector maps describing the symmetric (i.e., Euclidian and minimum in-water distances) and asymmetric (simulated propagule displacement) variables with genetic variation. This approach is more efficient at describing fine-scale spatial genetic structure than Mantel tests, as it partitions the contribution of many evolutionary processes across loci (Diniz-Filho et al. 2013). Briefly, the symmetric variables were transformed into distance-based Moran's eigenvector maps (dbMEM) (Dray et al. 2006) while the simulated probabilities of propagule displacement were transformed into an asymmetric eigenvector map (AEM) (Blanchet et al. 2011) with the R package adespatial v0.3-16 (Dray et al. 2022), as described in Xuereb et al. (2018). We ran a PCA on the Hellinger-transformed allele frequencies (Legendre and Gallagher 2001) and used the most explanatory components as response variables of the predictors, AEM and dbMEM, for the RDA. We identified the most explanatory variables with the R package vegan v2.5-7 (Oksanen et al. 2020) and used ANOVA with 1000 permutations to access the significance of the model and the contribution of each variable. These analyses were not performed for recent migration rates, as they were negligible (see Results).

Results

SNP calling, filtering and neutral SNP selection

We sequenced 1,582,998 reads for all samples obtained by our group, comprising the individuals sampled in the Western hemisphere and South Pacific islands, with 81.19% alignment rate with the reference genome. We retained 263,279 SNPs from this complete dataset. After the filtering steps and including only individuals sampled in the Southwest Atlantic basin, we kept 6,568 SNPs. We found 112, 1 and 241 outlier SNPs with pcadapt, Bayescan and LOSITAN, respectively, and 23 loci associated with each environmental variable on the LFMM analyses, on average. The most relevant environmental variable, associated with 35 SNPs, was the mean annual sea surface temperature. We identified 58 SNPs as putatively

under selection in at least three of these methods, and therefore kept 6,510 uncoupled neutral SNPs to the downstream analyses.

Population genetic structure

Both DAPC and admixture analyses showed two major populations (K = 2) of *R. mangle* on the Southwest Atlantic coast: one population in the north- and another south- of the northeastern extremity of South America (NEESA), henceforth regarded as 'north group' and 'south group', respectively. We found more admixed individuals in the north group on both independent analyses (Supplementary Figure 1 and Figure 1b). Considering a finer scale structure (K = 3 and K = 4) in the admixture analysis, we also could observe the two major groups, north and south, with more admixed individuals in the north (i.e., more unique genetic groups were rarely found in the south group). The F_{ST} between the north and south groups was significant ($F_{ST} = 0.032$, $P < 0.00001$), which indicates significant population structure between both groups. Only three pairwise F_{ST} values regarding the GPM sampling site were significant. We recognize that this result is likely an artifact due to the small sample size for this locality. With GPM excluded, 91% of the pairwise F_{ST} values were significant, ranging from 0.056 to 0.149 (Figure 1c). This north-south pattern was also recovered by effective migration surfaces found with EEMS, which also revealed a barrier to migration within the north group and greater gene flow within the south group (Figure 1d).

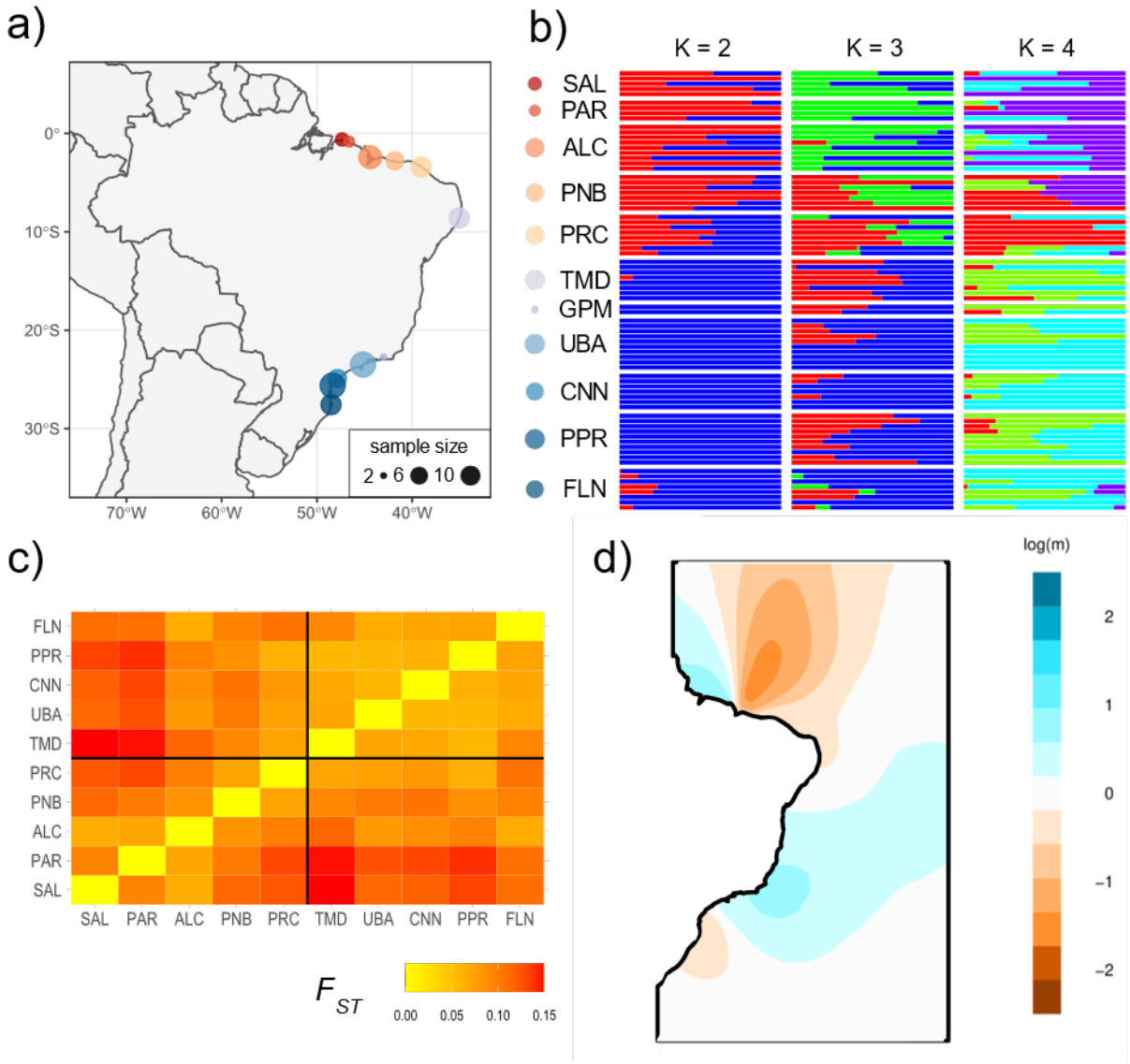

Figure 1. Sampling and population genetic structure of *Rhizophora mangle*. a) geographic distribution of the sampling sites along the Southwest Atlantic basin. Sample sizes are represented by the size of the circles and their colors denotes sampling sites. b) population genetic structure identified with admixture, with K = 2 - 4. Each line represents one individual, and each color represents an inferred ancestry. c) pairwise F_{ST} between all samples, excluding GPM. Warmer colors indicate higher F_{ST} values. Black lines split the sampling sites between the north and south groups identified in the population structure analyses. d) effective migration surface of log of the mean migration parameter *m*. Warmer colors denotes lower log(*m*). Acronyms for the sampling sites follows Table 1.

Migration rates

The recent migration rates estimated between samples were negligible, as none presented a confidence interval that did not include zero. The ancestral migration models that best fitted our data was the steppingstone model for the north group and the panmixia model for the south group (Table 2). Migration rates within south group were, in average, six times higher

than those within north group (6.286×10^{-3} and 1.162×10^{-3}, respectively) (Figure 2). The ancestral migration rates *between* both groups were two to three orders of magnitude smaller than the inferred migration rates *within* groups. Also, long-term migration estimates between groups revealed a 50% higher migration from south to north than the opposite direction (S→N: 1.525×10^{-5}; N→S: 9.687×10^{-6}). The highest ancestral migration rates inferred within each group was from ALC to SAL in the north group (7.275×10^{-3}) and from TMD to GPM in the south group (0.052).

Table 2. Within groups long-term migration models tested with fastsimcoal26. deltaL: difference between the obtained likelihood in the best run and the maximum possible likelihood for the model. AIC: Akaike information criterion. Best AIC values for each region are highlighted in bold.

	North Group		South Group	
	deltaL	AIC	deltaL	AIC
Steppingstone	1030.526	**15029.562**	4997.803	97369.966
Directional	1294.901	16271.054	4869.849	96820.716
Panmixia	1043.597	15113.756	4727.517	**96165.253**

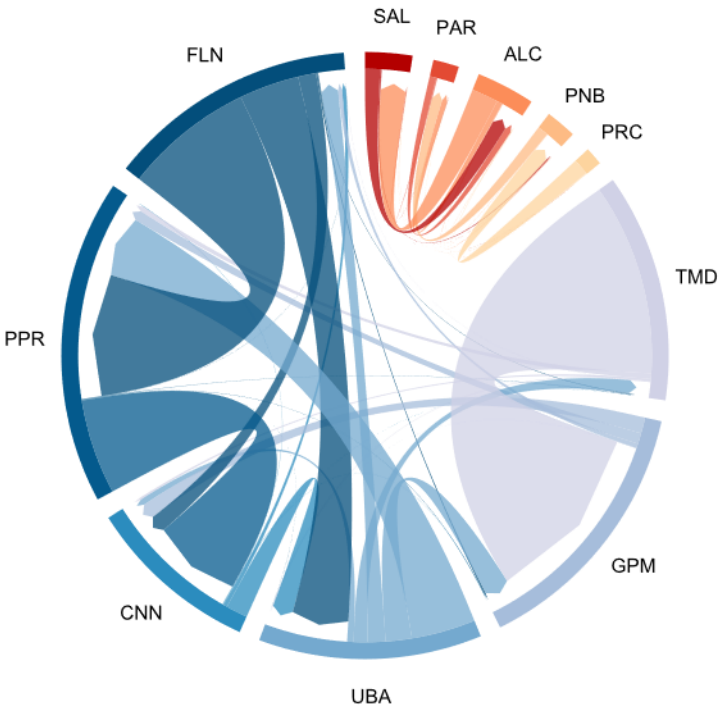

Figure 2. Within groups ancestral migration rates. Long-term migration rates inferred with fastsimcoal26 within each group are shown. Arrows points from one sampling site in direction of the inferred migration destination, and its width represents the intensity of migration. Between groups long-term migration rates are not shown. Acronyms for sampling sites follow Table 1.

Oceanic transport estimates

Adrift and OpenDrift analyses provided similar results (Mantel $r = 0.7$, $P < 0.0001$). Both showed a clear separation between north and south groups (Figure 3), without substantial exchange of particles (i.e., propagules) between groups. In Adrift analysis (Figure 3a), populations from the north group and TMD, which is located south to the NEESA, showed high rates of transport of particles from east to west. Probabilities of propagules drifting in the other direction were null, with the exception of the neighboring sites PAR and SAL. TMD site was the only one showing non null probabilities of transport to all other localities, with a higher probability of transport to sites of the north group (min = 6.6%; max = 23.2%; mean = 12%) than to those within south group (min = 0.2%; max = 1.2%; mean = 1%). TMD is also the only site that did not receive propagules from any of the other site, acting solely as a propagule donor. In the mechanistic simulation of propagule displacement with OpenDrift (Figure 3b), TMD is further isolated, and has only contributed to GPM site, with only ten propagules out of 100,000. Unlike the outcomes of Adrift, the east-to-west directionality of propagules trajectories within the north group was not observed. The overall propagule exchange between sites within the south group was 1.4x higher in average than the exchange between localities within the north group. Both mechanistic and probabilistic analyses highlighted the intense propagule exchange between SAL and PAR within the north group, and between PPR and CNN within the south group. Additionally, both methods showed higher probability of particle transport within the site of release, 56.5% for Adrift and 82.8% for OpenDrift. This difference is likely due to the assumptions of each method, like considering beaching only for the latter.

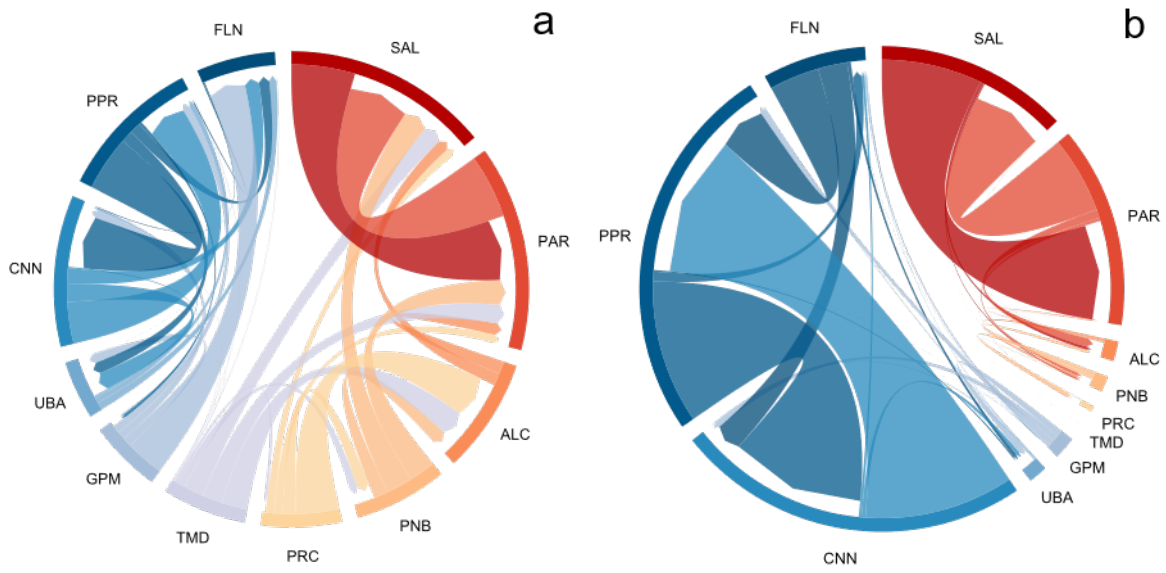

Figure 3. Oceanic transport estimates. a) probabilistic oceanic transport estimates with Adrift. b) mechanistic simulation of propagule displacement with OpenDrift. The arrows points in the direction of the propagule transit, and its width represents the intensity of the particle exchange. Self-pointing arrows were excluded from the representation. Acronyms for the sampling sites follows the notation on Table 1.

Drivers of isolation

We used the results obtained only with OpenDrift to test the effects of oceanic currents, because we observed a significant correlation between Adrift and OpenDrift outcomes. We found evidence for isolation by distance based on the correlation between the Euclidian (Mantel r = -0.189, P = 0.029) and minimum in-water distances (Mantel r = -0.207, P = 0.008) with the inferred ancestral migration rates. The correlation between the propagule displacement simulation with these rates was higher (Mantel r = 0.273, P = 0.048), suggesting a stronger effect of oceanography on migration.

Regarding the RDA analyses, we retained four axes of the PCA with the Hellinger-transformed allele frequencies, which cumulatively explained 56.28% of the total neutral genetic variance. The selection of asymmetrical explanatory variables (i.e., the AEM obtained with the propagule displacement simulation results) retained one AEM variable (AEM1) (Figure 4a). The RDA considering AEM1 and the four PCs retained had a coefficient of determination (adjusted R^2) of 8.1% (P = 0.03). We identified one significant Euclidian dbMEM (dbMEM1) (Figure 4b) and two in-water dbMEMs (dbMEM1 and dbMEM10) (Figure

4c and d). The RDA regarding the selected dbMEM variables showed significant coefficients of determination (for Euclidian distances: R^2 = 6.7%, P = 0.045; for in-water distances: R^2 = 20.3%, P = 0.013). The retention of the first eigenvector map for AEM, Euclidian and in-water dbMEM indicate a broad-scale spatial structure, because eigenvector maps are increasingly specific in the spatial-scale they explain.

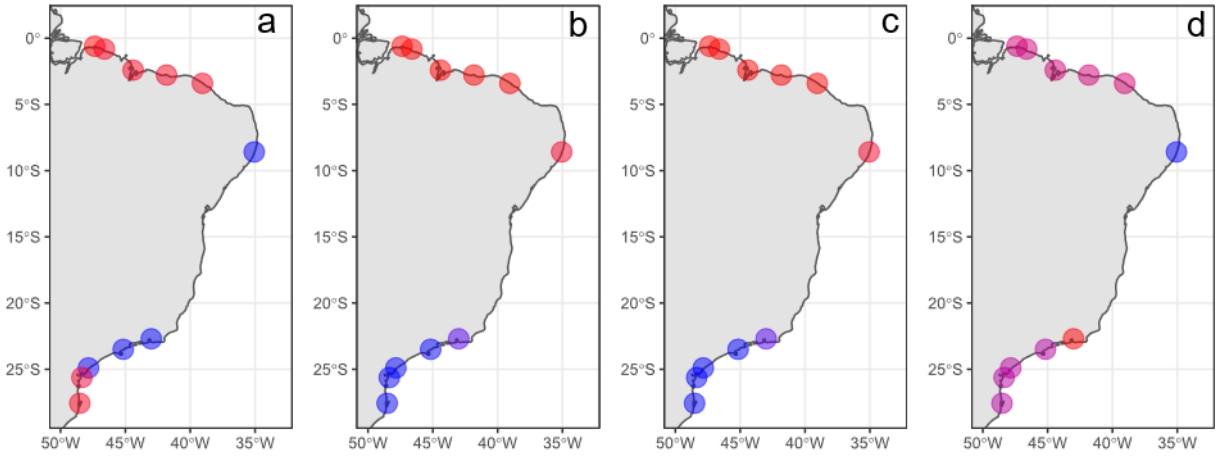

Figure 7. Visual representation of the significative eingenvector maps retained for the RDA analysis. a) AEM1; b) Euclidean dbMEM1; c) in-water dbMEM1; d) in-water dbMEM10. For each individual map, similar colors represents similar eigenvector map values.

Discussion

We recovered the north-south population genetic structure found for *R. mangle* in previous studies (Pil et al. 2011; Takayama et al. 2013; Francisco et al. 2018) in the Southwest Atlantic coast using genomic tools. Recovering this pattern using thousands of single-base markers, which may be under different evolutionary regimes than microsatellites used in previous works, strengthens the evidence for such structure. Our findings based on multiple lines of evidence were consistent with this pattern. We observed low long-term migration rates between north and south groups, low probability of oceanic transport between groups, and different migration patterns within each group. Our results show that both geographic and oceanographic distances are crucial factors to explain the neutral genetic variation of mangrove populations.

Large-scale connectivity

At large geographic scale, our results based on 6,510 unlinked neutral SNPs revealed a north-south population genetic structure. We observed the subdivision between north and south groups with more admixed individuals in the former with multiple analyses. This pattern was recovered with the model-based inference of individual ancestry with admixture, a multivariate clustering of related individuals (DAPC), the genetic distance among samples (pairwise F_{ST}) and the effective migration surfaces (EEMS). Additionally, this structure is recovered at smaller scales (K = 3 and K = 4 in the admixture analysis), indicating that this is a major pattern of *R. mangle* population genetic structure in the Southwest Atlantic basin. The geographic positioning of the barrier to gene flow within the region of the NEESA was also compatible across methods. Resembling patterns of organization of the genetic variation were previously reported for *R. mangle* (Pil et al. 2011; Francisco et al. 2018) and other coastal plants (Mori et al. 2015; Cruz et al. 2019, 2020; Da Silva et al. 2021). Additionally, the EEMS results revealed a smooth westward population differentiation in the north group, mirroring a previous study that used microsatellites (Francisco et al., 2018). The observation of similar patterns with a considerably larger number of molecular markers (~6,500 SNPs) compared to previous studies conducted with less than 10 microsatellites (Pil et al. 2011; Francisco et al. 2018) may be interpreted as a consistent evidence of limited gene flow at large geographic scales.

Our analyses showed that contemporary migration is rare or absent, whereas rates of long-term migration were not only non-negligible but largely asymmetrical. We observed low levels of historical migration between groups, which supports the population genetic structure found. Our findings also indicated a 1.5x higher ancestral migration rate from south-to-north relative to north-to-south, which is consistent with the higher number of admixed individuals in the north group. This pattern could be explained by the prevalent oceanic currents in the studied region; the split of the South Equatorial Current into the North Brazilian Current and the Brazilian Current would separate the north and south groups. Also, the weaker Brazilian Current would allow the occasional northward dispersal more often than the stronger North Brazilian Current would allow southward dispersal (Lumpkin and Johnson 2013). These results coupled with the population genetic structure results allow us to reject the null hypothesis of panmixia (H_0) and H_1, which assumes small-scale population structure leading to isolated

populations, since we observed a predominant large-scale structure, with non-negligible connectivity between sampling sites within each group.

The overall incongruence of the results obtained with BA3-SNPs and fastsimcoal26 is likely an outcome of the rarity of LDD events (Nathan 2006), even for organisms such as mangroves, which are capable of transoceanic dispersal (e.g. Mori et al., 2015, 2021; Nettel & Dodd, 2007; Ngeve et al., 2021; Takayama et al., 2021). *R. mangle* populations would remain majorly isolated, and rare LDD events would contribute to the mixing of populations. The ancestral migration rates inferred were low (mean 4.02×10^{-3}), indicating that these admixture events are rare even within the inferred genetic groups (south and north). Over time, this admixture would become evident, but in a few-generations scale, it would not be possible to identify this phenomenon.

Likewise, the mechanistic and probabilistic propagule displacement simulations revealed a clear distinction between north and south groups. Both showed that propagules most likely remain within its release group. One key difference between the findings obtained with Adrift and OpenDrift was the probability of transit away from the release site, which was higher for the former. Another difference we observed between the results of these biophysical oceanographic methods regards the TMD site. This south group site is geographically closed to the NEESA and to the split of the South Equatorial Current (Lumpkin and Johnson 2013). The analyses with Adrift showed that particles released from TMD can reach all remaining sites in both groups. Contrastingly, OpenDrift analyses showed a sharper distinction, in which propagules released from TMD stranded only at the GPM site.

Such contrasts may be understood by the underlying differences between methodologies. Adrift, which relies on surface drifter trajectories spanning from 1979 to 2013, calculates probabilities of transit of particles in a transition matrix (van Sebille 2014). Conversely, OpenDrift is deterministic; a particle released in a given location and time will always have the same trajectory (Dagestad et al. 2018). Furthermore, for the OpenDrift analyses, we simulated the release of 10^6 particles, evenly released for ten years, from 2010 to 2020. These methodological differences allow us to interpret the outcomes of each method as complementary timeframes and time scales. Our analyses with OpenDrift considered a narrower and more recent timeframe and generated particle trajectories patterns that indicated an absence of dispersal between groups. Contrastingly, Adrift outcomes revealed drift patterns

that suggest that long-term propagule dispersal from south group to north group is not only a possible, but a plausible phenomenon. These findings are in line with the population genetic structure and asymmetric long-term migration patterns and the negligible contemporary migration rates. Interpreted together, they are consistent with LDD in *R. mangle*.

Long distance dispersal events are mostly infrequent, but have important consequences for population dynamics and evolution (Cain et al. 2000; Nathan et al. 2008; Kremer et al. 2012; Jordano 2017). A combined interpretation of lines of evidence regarding oceanographic physical modelling and molecular data allows us to bridge ecological processes of dispersal, from emigration and transfer to immigration (Van der Stocken et al. 2019b), with its genetic outcomes at genomic scale. This combination also allowed us to unveil connectivity patterns at finer spatial scales.

Small-scale connectivity

Our results suggest contrasting modes of dispersal within each group based on multiple sources of information. A higher gene flow within the south group is evident from the effective migration surface. Within this group, we also observed 6x higher ancestral migration rates and 1.4x higher displacement rates of propagules estimated with OpenDrift, compared to those estimated for the north group. Complementarily, model testing with fastsimcoal26 indicated that a steppingstone model better fitted our genetic data for the north group whereas panmixia model best explained the genetic variation of the south group. This was corroborated by the OpenDrift analyses. It would be reasonable to expect neighboring sites to extensively exchange propagules, but, within the north group, the rates of exchange between neighbors were higher in comparison to the south group. The ratio of average number of propagules transported to neighboring sites over the average number of propagules transported do non-neighboring sites was 4.7 for the north group and 3.4 for the south group. These results together emphasize the higher connectivity within the south group compared to the north group and highlight that the connectivity patterns within each region is structurally different. Therefore, these groups are not only highly differentiated based on different molecular markers (Pil et al. 2011; Takayama et al. 2013; Francisco et al. 2018), they also disperse differently.

Drivers of isolation

Oceanic currents have been used to explain the genetic divergence between north and south groups in mangrove trees (Pil et al. 2011; Mori et al. 2015; Cruz et al. 2019, 2020; Da Silva et al. 2021) and other coastal plants (Takayama et al. 2008). Because this pattern of neutral population genetic structure is consistent across independent lineages, it is reasonable to argue that a shared extrinsic factor, or a set of common abiotic factors, independently shapes the connectivity of these coastal species. Using a landscape genomics approach, it has been recently shown that the neutral genetic variation of the mangrove tree *Avicennia schaueriana* is largely driven by the barrier created by the bifurcation of the South Equatorial Current and by geographic distances (Da Silva et al. 2021). In that study, this oceanographic bifurcation was treated as an absolute and static barrier and, therefore, it could not address how directionality, strength and variability of ocean currents influence mangroves' dispersal (Da Silva et al. 2021). Here, the use of oceanographic modelling and genomic data under an integrated statistical framework allowed us to take a step further to provide more realistic insights into the effects of oceanic currents on the connectivity of *R. mangle,* and more broadly, of mangrove and coastal plant species.

Mantel tests showed that spatial distances play an important role shaping the long-term migration of *R. mangle* (Euclidian distance: Mantel r = -0.189; minimum distance in-water: Mantel r = -0.207). However, a stronger correlation was observed when propagule displacement rates were used as a predictor of ancestral migration inferred with fastsimcoal26 (Mantel r = 0.273). Accordingly, the RDA results showed that both geography and the direction of ocean currents influence the spatial patterns of long-term migration. Both symmetrical (i.e., Euclidian and in-water dbMEMs) and asymmetrical (i.e., AEM, derived from propagule displacement analyses) eigenfunctions retained describe a broad spatial scale structure, accounting to the north-south population genetic divergence (Figure 4a, b and c). We did not recover fine scale structure with our eigenvector maps. It indicates that spatial distances and oceanic currents play a greater role separating both groups than finer-scale connectivity patterns *within* each group. In fact, based on oceanic currents alone (Lumpkin and Johnson 2013), one could expect greater east-to-west migration rates and propagule displacement. We only found this pattern with Adrift analyses. We argue that other factors, such as coastal regimes, pollen dispersal and shoreline geomorphology are likely more relevant to short-to-medium scales (i.e., from tens to few

hundreds of kilometers) connectivity of *R. mangle.* Such near-shore processes could influence the immigration stage of propagule dispersal filtering the access, retention and recruitment of seedlings (Van der Stocken et al. 2019b). To describe the dynamics of connectivity patterns at fine scales and to translate them across scales, future studies with complementary sampling resolutions, from landscape to biogeographic scales, are needed.

The last eigenfunction retained, dbMEM10 for the minimum in-water distance, showed a structure where TMD is isolated from the other localities (Figure 4d). As previously discussed, TMD is at an interesting geographic spot, at the border of both groups. It is associated with the south group based on population genetic structure analyses (admixture, DAPC and EEMS) and on propagule displacement simulations. Conversely, it is associated with the north group in the symmetric in-water (dbMEM1) and Euclidean (dbMEM1) eigenfunctions. It also may be positioned at an intermediate or isolated status regarding the Adrift analyses and the in-water dbMEM10 eigenfunction. Jointly, these findings indicate that TMD is genetically assigned to the south group but can possibly function as a bridge for LDD events that maintain the admixture between both groups, mainly north to the NEESA.

The discrepancies between the results of Mantel tests and RDA, for instance, suggest that the role played by oceanic currents is more relevant at larger scales compared to finer scales (i.e., within groups). Mantel tests provide a global summary of effective connectivity (migration rates), revealing large-scale patterns, while eigenvector maps enable the partition of genetic variation in multiple loci, revealing fine-scale processes (Dray et al. 2006; Diniz-Filho et al. 2013). The combined interpretation of different methods is necessary to identify processes that operate at different scales, as the stochasticity of dispersal dynamics at smaller scales hinders the identification of general patterns and tendencies across scales (Chave 2013).

Overall, our findings provide evidence to reject H_0 and H_1. Additionally, they allow one to reject H_3, which assumes that oceanic currents are the only driver of dispersal of *R. mangle* propagules, because we did not observe a match between genetic and oceanographic patterns. Thus, based on our isolated and combined findings, we could not reject our third hypothesis (H_2), which stated that the connectivity of *R. mangle* would be explained by multiple factors. Although we observed that oceanic currents are important drivers of isolation in a dominant mangrove tree, we could not rule out the influence of geographic and in-water distances.

Our study showcases how the combination of genetic-based and biophysical oceanographic models improves the interpretation of connectivity patterns across temporal and spatial scales. The use of complementary statistical methods to assess to what extent spatial and oceanographic features explain the genomic variation allowed a broader understanding of how ecological and evolutionary processes shape mangrove connectivity in the Southwest Atlantic basin. More broadly, we expect this work to contribute disproportionally to the seascape genetics and genomics literature because it focuses on coastal plants, a functional group with few studies, and it was carried out in one of the "very underrepresented" areas of the globe, the Southwest Atlantic basin (Jahnke and Jonsson 2022).

Perspectives

Our genetic-based findings largely support the genetic structure patterns described in previous studies on *R. mangle* (Pil et al. 2011; Takayama et al. 2013; Francisco et al. 2018) and other coastal plants (Takayama et al. 2008; Mori et al. 2015; Cruz et al. 2019, 2020; Da Silva et al. 2021). However, there are differences across taxa. For instance, *Avicennia*, also a mangrove species, and *H. pernambucensis,* a coastal plant that grows inland of mangrove forests and along brackish rivers, present sharper genetic breaks between groups found north and south of the NEESA (Takayama et al. 2008; Mori et al. 2015; Cruz et al. 2019, 2020; Da Silva et al. 2021) compared to *R. mangle.* Remarkably, *Laguncularia racemosa,* a mangrove species whose geographic range largely overlaps with the one *R. mangle* presents, showed a homogenous distribution of the genetic variation across the Southwest Atlantic coast (Sereneski-Lima et al. 2021), unlike its counterparts. It reinforces that species-specific traits, like propagules' flotation or longevity, also contribute to the connectivity of mangrove plants (Van der Stocken et al. 2019b), which remains an open avenue for future investigations.

As climate rapidly changes, so do oceans. Recent evidence indicates that future environmental conditions under representative concentration pathway 8.5 by 2100 will likely change dispersal potential of mangroves. Changes in sea surface salinity, density and temperature of waters bordering mangrove forests are expected to make LDD events even rarer and promote short-distances dispersal (Van der Stocken et al. 2022). Because north and south groups are genetically divergent and possess contrasting dispersal patterns, in future conditions, plants from both groups will likely face novel in-transit challenges, with ecological and evolutionary consequences.

Conclusion

The combination of genomic-scale data with biophysical oceanographic simulations is in line with the hypothesis that oceanic currents, spatial and in-water distances play a role as drivers of dispersal of *Rhizophora mangle.* Although these distances are important factors that explain the species' connectivity, considering the non-linear, dynamic, and asymmetric nature of oceanic currents provided a broader perspective on the connectivity of coastal plants across scales. As sea surface properties change, dispersal will likely be affected, with potentially major ecological and evolutionary consequences. The realism provided by the mechanistic explanation of biophysical models to the population genetic structure and migration patterns we observed adds to the increasing literature regarding the seascape genetics and genomics of coastal plants.

Acknowledgements

The authors are grateful to PR Laborda, SCS Andrade, AG Nazareno, MPP Romeiro and T Tjui-Yeuw for the constructive critics and suggestions on earlier versions of this manuscript and MC Almeida for assistance with preliminary analysis. This study was supported by research awards granted by the Brazilian National Council for Scientific and Technological Development (CNPq) and Japan Society for the Promotion of Science (JSPS) to GMM (CNPq 448286/2014-9) and to TK (JSPS KAKENHI 25290080 and 17H01414). Also, we thank São Paulo Research Foundation (FAPESP) for the research fellowships to AGM (FAPESP 18/02655-8 and 2020/07967-8) and GMM (FAPESP 13/08086-1 and 14/22821-9). This research was supported by resources supplied by the UNESP Center for Scientific Computing (NCC/GridUNESP). Additionally, this study was financed in part by the Coordenação de Aperfeiçoamento de Pessoal de Nível Superior - Brasil (CAPES) - Finance Code 001.

References

Aho, K., D. Derryberry, and T. Peterson. 2014. Model selection for ecologists: the worldviews of AIC and BIC. Ecology 95:631–636.

Alexander, D. H., J. Novembre, and K. Lange. 2009. Fast model-based estimation of ancestry in unrelated individuals. Genome Res. 19:1655–1664.

Antao, T., A. Lopes, R. J. Lopes, A. Beja-Pereira, and G. Luikart. 2008. LOSITAN: A workbench to detect molecular adaptation based on a Fst-outlier method. BMC Bioinformatics 9:323.

Assis, J., N. Castilho Coelho, F. Alberto, M. Valero, P. Raimondi, D. Reed, and E. Alvares Serrão. 2013. High and distinct range-edge genetic diversity despite local bottlenecks. PLoS One 8:e68646.

Baird, N. A., P. D. Etter, T. S. Atwood, M. C. Currey, A. L. Shiver, Z. A. Lewis, E. U. Selker, W. A. Cresko, and E. A. Johnson. 2008. Rapid SNP discovery and genetic mapping using sequenced RAD markers. PLoS One 3:1–7.

Beaumont, M. A., and R. A. Nichols. 1996. Evaluating loci for use in the genetic analysis of population structure. Proc. R. Soc. London. Ser. B Biol. Sci. 263:1619–1626.

Bergmann, P. J., and E. J. McElroy. 2014. Many-to-many mapping of phenotype to performance: an extension of the F-matrix for studying functional complexity. Evol. Biol. 41:546–560.

Bertola, L. D., J. T. Boehm, N. F. Putman, A. T. Xue, J. D. Robinson, S. Harris, C. C. Baldwin, I. Overcast, and M. J. Hickerson. 2020. Asymmetrical gene flow in five co-distributed syngnathids explained by ocean currents and rafting propensity. Proc. R. Soc. B Biol. Sci. 287.

Blanchet, F. G., P. Legendre, R. Maranger, D. Monti, and P. Pepin. 2011. Modelling the effect of directional spatial ecological processes at different scales. Oecologia 166:357–368.

Bolger, A. M., M. Lohse, and B. Usadel. 2014. Trimmomatic: a flexible trimmer for Illumina sequence data. Bioinformatics 30:2114–2120.

Bonjean, F., and G. S. E. Lagerloef. 2002. Diagnostic model and analysis of the surface currents in the tropical Pacific Ocean. J. Phys. Oceanogr. 32:2938–2954.

Bullock, J. M., and R. Nathan. 2008. Plant dispersal across multiple scales: linking models and reality. J. Ecol. 96:567–568.

Cain, M. L. M. L., B. G. Milligan, and A. E. A. E. Strand. 2000. Long-distance seed dispersal in plant populations. Am. J. … 87:1217–1227.

Canty, S. W. J., J. P. Kennedy, G. Fox, K. Matterson, V. L. González, M. L. Núñez-Vallecillo, R. F. Preziosi, and J. K. Rowntree. 2022. Mangrove diversity is more than fringe deep. Sci. Rep. 12:1695.

Cayuela, H., Q. Rougemont, J. G. Prunier, J. S. Moore, J. Clobert, A. Besnard, and L. Bernatchez. 2018. Demographic and genetic approaches to study dispersal in wild animal populations: A methodological review. Mol. Ecol. 27:3976–4010.

Cerón-Souza, I., E. Rivera-Ocasio, E. Medina, J. A. Jiménez, W. O. McMillan, and E. Bermingham. 2010. Hybridization and introgression in new world red mangroves, *Rhizophora* (Rhizophoraceae). Am. J. Bot. 97:945–957.

Chave, J. 2013. The problem of pattern and scale in ecology: What have we learned in 20 years? Ecol. Lett. 16:4–16.

Cruz, M. V., G. M. Mori, D. H. Oh, M. Dassanayake, M. I. Zucchi, R. S. Oliveira, and A. P. de Souza. 2020. Molecular responses to freshwater limitation in the mangrove tree *Avicennia germinans* (Acanthaceae). Mol. Ecol. 29:344–362.

Cruz, M. V., G. M. Mori, C. Signori-Müller, C. C. da Silva, D.-H. Oh, M. Dassanayake, M. I. Zucchi, R. S. Oliveira, and A. P. de Souza. 2019. Local adaptation of a dominant coastal tree to freshwater availability and solar radiation suggested by genomic and ecophysiological approaches. Sci. Rep. 9:19936.

Da Silva, M. F., M. V. Cruz, J. D. D. Vidal Júnior, M. I. Zucchi, G. M. Mori, and A. P. De Souza. 2021. Geographical and environmental contributions to genomic divergence in mangrove forests. Biol. J. Linn. Soc. 132:573–589.

Dagestad, K.-F., J. Röhrs, Ø. Breivik, and B. Ådlandsvik. 2018. OpenDrift v1.0: a generic framework for trajectory

modelling. Geosci. Model Dev. 11:1405–1420.

Danecek, P., A. Auton, G. Abecasis, C. A. Albers, E. Banks, M. A. DePristo, R. E. Handsaker, G. Lunter, G. T. Marth, S. T. Sherry, G. McVean, and R. Durbin. 2011. The variant call format and VCFtools. Bioinformatics 27:2156–2158.

Diniz-Filho, J. A. F., J. V. B. P. L. Diniz, T. F. Rangel, T. N. Soares, M. P. de C. Telles, R. G. Collevatti, and L. M. Bini. 2013. A new eigenfunction spatial analysis describing population genetic structure. Genetica 141:479–489.

Dray, S., D. Bauman, F. G. Blanchet, D. Borcard, S. Clappe, G. Guenard, T. Jombart, G. Larocque, P. Legendre, N. Madi, and H. H. Wagner. 2022. adespatial: multivariate multiscale spatial analysis. R package.

Dray, S., P. Legendre, and P. R. Peres-Neto. 2006. Spatial modelling: a comprehensive framework for principal coordinate analysis of neighbour matrices (PCNM). Ecol. Modell. 196:483–493.

Driscoll, D. A., S. C. Banks, P. S. Barton, K. Ikin, P. Lentini, D. B. Lindenmayer, A. L. Smith, L. E. Berry, E. L. Burns, A. Edworthy, M. J. Evans, R. Gibson, R. Heinsohn, B. Howland, G. Kay, N. Munro, B. C. Scheele, I. Stirnemann, D. Stojanovic, N. Sweaney, N. R. Villaseñor, and M. J. Westgate. 2014. The trajectory of dispersal research in conservation biology. Systematic Review. PLoS One 9:e95053.

EXCOFFIER, L., and H. E. L. LISCHER. 2010. Arlequin suite ver 3.5: a new series of programs to perform population genetics analyses under Linux and Windows. Mol. Ecol. Resour. 10:564–567.

Excoffier, L., N. Marchi, D. A. Marques, R. Matthey-Doret, A. Gouy, and V. C. Sousa. 2021. fastsimcoal2 : demographic inference under complex evolutionary scenarios. Bioinformatics 37:4882–4885.

Fick, S. E., and R. J. Hijmans. 2017. WorldClim 2: new 1-km spatial resolution climate surfaces for global land areas. Int. J. Climatol. 37:4302–4315.

Foll, M., and O. Gaggiotti. 2008. A genome-scan method to identify selected loci appropriate for both dominant and codominant markers: a bayesian perspective. Genetics 180:977–993.

Francisco, P. M., G. M. Mori, F. M. Alves, E. V. Tambarussi, and A. P. de Souza. 2018. Population genetic structure, introgression, and hybridization in the genus *Rhizophora* along the Brazilian coast. Ecol. Evol. 8:3491–3504.

François, O., H. Martins, K. Caye, and S. D. Schoville. 2016. Controlling false discoveries in genome scans for selection. Mol. Ecol. 25:454–469.

Frichot, E., S. D. Schoville, G. Bouchard, and O. Franc. 2013. Testing for associations between loci and environmental gradients using latent factor mixed models. 30:1687–1699.

Geng, Q., Z. Wang, J. Tao, M. K. Kimura, H. Liu, T. Hogetsu, and C. Lian. 2021. Ocean currents drove genetic structure of seven dominant mangrove species along the coastlines of southern china. Front. Genet. 12.

Grünwald, N. J., S. E. Everhart, B. J. Knaus, and Z. N. Kamvar. 2017. Best practices for population genetic analyses. Phytopathology 107:1000–1010.

Hasan, S., L. Triest, S. Afrose, and D. J. R. De Ryck. 2018. Migrant pool model of dispersal explains strong connectivity of *Avicennia officinalis* within Sundarban mangrove areas: Effect of fragmentation and replantation. Estuar. Coast. Shelf Sci. 214:38–47. Elsevier.

Hays, G. C. 2017. Ocean currents and marine life. Curr. Biol. 27:R470–R473. Elsevier.

Hays, G. C., L. C. Ferreira, A. M. M. Sequeira, M. G. Meekan, C. M. Duarte, H. Bailey, F. Bailleul, W. D. Bowen, M. J. Caley, D. P. Costa, V. M. Eguíluz, S. Fossette, A. S. Friedlaender, N. Gales, A. C. Gleiss, J. Gunn, R. Harcourt, E. L. Hazen, M. R. Heithaus, M. Heupel, K. Holland, M. Horning, I. Jonsen, G. L. Kooyman, C. G. Lowe, P. T. Madsen, H. Marsh, R. A. Phillips, D. Righton, Y. Ropert-Coudert, K. Sato, S. A. Shaffer, C. A. Simpfendorfer, D. W. Sims, G. Skomal, A. Takahashi, P. N. Trathan, M. Wikelski, J. N. Womble, and M. Thums. 2016. Key questions in marine megafauna movement ecology. Trends Ecol. Evol. 31:463–475. Elsevier Ltd.

Hodel, R. G. J., L. L. Knowles, S. F. McDaniel, A. C. Payton, J. F. Dunaway, P. S. Soltis, and D. E. Soltis. 2018. Terrestrial species adapted to sea dispersal: Differences in propagule dispersal of two Caribbean mangroves. Mol. Ecol. 27:4612–4626.

Jahnke, M., and P. R. Jonsson. 2022. Biophysical models of dispersal contribute to seascape genetic analyses. Philos. Trans. R. Soc. B Biol. Sci. 377.

Jombart, T., and I. Ahmed. 2011. adegenet 1.3-1: new tools for the analysis of genome-wide SNP data. Bioinformatics 27:3070–3071.

Jombart, T., S. Devillard, and F. Balloux. 2010. Discriminant analysis of principal components: a new method for the analysis of genetically structured populations. BMC Genet. 11:94.

Jordano, P. 2017. What is long-distance dispersal? And a taxonomy of dispersal events. J. Ecol. 105:75–84.

Kremer, A., O. Ronce, J. J. Robledo-Arnuncio, F. Guillaume, G. Bohrer, R. Nathan, J. R. Bridle, R. Gomulkiewicz, E. K. Klein, K. Ritland, A. Kuparinen, S. Gerber, and S. Schueler. 2012. Long-distance gene flow and adaptation of forest trees to rapid climate change. Ecol. Lett. 15:378–392.

Lalire, M., and P. Gaspar. 2019. Modeling the active dispersal of juvenile leatherback turtles in the North Atlantic Ocean. Mov. Ecol. 7:1–17. Movement Ecology.

Langmead, B., and S. L. Salzberg. 2012. Fast gapped-read alignment with Bowtie 2. Nat. Methods 9:357–359.

Legendre, P., and E. D. Gallagher. 2001. Ecologically meaningful transformations for ordination of species data. Oecologia 129:271–280.

Li, H. 2011. A statistical framework for SNP calling, mutation discovery, association mapping and population genetical parameter estimation from sequencing data. Bioinformatics 27:2987–2993.

Liu, J., A. J. Lindstrom, Y. Chen, R. Nathan, and X. Gong. 2021. Congruence between ocean-dispersal modelling and phylogeography explains recent evolutionary history of *Cycas* species with buoyant seeds. New Phytol. 232:1863–1875.

Lowe, W. H., R. P. Kovach, and F. W. Allendorf. 2017. Population Genetics and Demography Unite Ecology and Evolution. Trends Ecol. Evol. 32:141–152. Elsevier Ltd.

Lumpkin, R., and G. C. Johnson. 2013. Global ocean surface velocities from drifters: Mean, variance, El Niño-Southern Oscillation response, and seasonal cycle. J. Geophys. Res. Ocean. 118:2992–3006.

Luu, K., E. Bazin, and M. G. B. Blum. 2017. pcadapt: an R package to perform genome scans for selection based on principal component analysis. Mol. Ecol. Resour. 17:67–77.

Mantel, N. 1967. The detection of disease clustering and a generalized regression approach. Cancer Res. 27:209–20.

Martin, M. 2011. Cutadapt removes adapter sequences from high-throughput sequencing reads. EMBnet.journal 17:10.

Mori, G. M., A. G. Madeira, M. V. Cruz, Y. Tsuda, K. Takayama, Y. Matsuki, Y. Suyama, T. Iwasaki, A. P. de Souza, M. I. Zucchi, and T. Kajita. 2021. Testing species hypotheses in the mangrove genus *Rhizophora* from the Western hemisphere and South Pacific islands. Estuar. Coast. Shelf Sci. 248.

Mori, G. M., M. I. Zucchi, and A. P. Souza. 2015. Multiple-geographic-scale genetic structure of two mangrove tree species: The roles of mating system, hybridization, limited dispersal and extrinsic factors. PLoS One 10:1–23.

Mussmann, S. M., M. R. Douglas, T. K. Chafin, and M. E. Douglas. 2019. BA3-SNPs: Contemporary migration reconfigured in BayesAss for next-generation sequence data. Methods Ecol. Evol. 10:1808–1813.

Narasimhan, V., P. Danecek, A. Scally, Y. Xue, C. Tyler-Smith, and R. Durbin. 2016. BCFtools/RoH: a hidden Markov model approach for detecting autozygosity from next-generation sequencing data. Bioinformatics

32:1749–1751.

Nathan, R. 2006. Long distance dispersal of plants. 313:786–788.

Nathan, R., G. Perry, J. T. Cronin, A. E. Strand, M. L. Cain, and M. L. Methods. 2003. Methods for estimating long-distance dispersal. Oikos 103:261–273.

Nathan, R., F. M. Schurr, O. Spiegel, O. Steinitz, A. Trakhtenbrot, and A. Tsoar. 2008. Mechanisms of long-distance seed dispersal. Trends Ecol. Evol. 23:638–647.

Nettel, A., and R. S. Dodd. 2007. Drifting propagules and receding swamps: Genetic footprints of mangrove recolonization and dispersal along tropical coasts. Evolution (N. Y). 61:958–971.

Ngeve, M. N., N. Koedam, and L. Triest. 2021. Genotypes of *Rhizophora* propagules from a non-mangrove beach provide evidence of recent long-distance dispersal. Front. Conserv. Sci. 2.

Ngeve, M. N., T. Van der Stocken, T. Sierens, N. Koedam, and L. Triest. 2017. Bidirectional gene flow on a mangrove river landscape and between-catchment dispersal of *Rhizophora racemosa* (Rhizophoraceae). Hydrobiologia 790:93–108. Springer International Publishing.

Ngeve, M. N., T. Vanderstocken, D. Menemenlis, N. Koedam, and L. Triest. 2016. Contrasting effects of historical sea level rise and contemporary ocean currents on regional gene flow of *Rhizophora racemosa* in eastern atlantic mangroves. PLoS One 11:1–24.

Nikolic, N., I. Montes, M. Lalire, A. Puech, N. Bodin, S. Arnaud-Haond, S. Kerwath, E. Corse, P. Gaspar, S. Hollanda, J. Bourjea, W. West, and S. Bonhommeau. 2020. Connectivity and population structure of albacore tuna across southeast Atlantic and southwest Indian Oceans inferred from multidisciplinary methodology. Sci. Rep. 10:15657.

Obst, M. 2017. Global tide variables. Swedish National Data Service.

Oksanen, J., F. G. Blanchet, M. Friendly, R. Kindt, P. Legendre, D. McGlinn, P. R. Minchin, R. B. O'Hara, G. L. Simpson, P. Solymos, M. H. H. Stevens, E. Szoecs, and H. Wagner. 2020. vegan: community ecology package. R package.

Petkova, D., J. Novembre, and M. Stephens. 2015. Visualizing spatial population structure with estimated effective migration surfaces. Nat. Genet. 48:94–100.

Pil, M. W. W., M. R. T. T. R. T. Boeger, V. C. C. Muschner, M. R. R. Pie, A. Ostrensky, and W. A. A. Boeger. 2011. Postglacial north-south expansion of populations of *Rhizophora mangle* (Rhizophoraceae) along the Brazilian coast revealed by microsatellite analysis. Am. J. Bot. 98:1031–1039.

Rochette, N. C., and J. M. Catchen. 2017. Deriving genotypes from RAD-seq short-read data using Stacks. Nat. Publ. Gr. 12:2640–2659. Nature Publishing Group.

Sbrocco, E. J., and P. H. Barber. 2013. MARSPEC: ocean climate layers for marine spatial ecology. Ecology 94:979–979.

Sereneski-Lima, C., R. A. Baggio, M. W. Pil, M. R. Torres Boeger, and W. A. Boeger. 2021. Historical and contemporary factors affect the genetic diversity and structure of *Laguncularia racemosa* (L.) Gaertn, along the western Atlantic coast. Estuar. Coast. Shelf Sci. 249:107055. Elsevier Ltd.

Shafer, A. B. A., J. M. Northrup, M. Wikelski, G. Wittemyer, and J. B. W. Wolf. 2016. Forecasting ecological genomics: high-tech animal instrumentation meets high-throughput sequencing. PLoS Biol. 14.

Slatkin, M. 1995. A measure of population subdivision based on microsatellite allele frequencies. Genetics 139:457–462.

Smith, T. M., P. H. York, B. R. Broitman, M. Thiel, G. C. Hays, E. van Sebille, N. F. Putman, P. I. Macreadie, and C. D. H. Sherman. 2018. Rare long-distance dispersal of a marine angiosperm across the Pacific Ocean. Glob. Ecol. Biogeogr. 27:487–496.

Takayama, K., M. Tamura, Y. Tateishi, E. L. Webb, and T. Kajita. 2013. Strong genetic structure over the American continents and transoceanic dispersal in the mangrove genus *Rhizophora* (Rhizophoraceae) revealed by broad- scale nuclear and chloroplast DNA analysis. Am. J. Bot. 100:1191–1201.

Takayama, K., Y. Tateishi, and T. Kajita. 2021. Global phylogeography of a pantropical mangrove genus *Rhizophora*. Sci. Rep. 11:7228.

Takayama, K., Y. Tateishi, J. Murata, and T. Kajita. 2008. Gene flow and population subdivision in a pantropical plant with sea-drifted seeds *Hibiscus tiliaceus* and its allied species: Evidence from microsatellite analyses. Mol. Ecol. 17:2730–2742.

Tomlinson, P. B. 2016. The Botany of Mangroves. Cambridge University Press.

Travis, J. M. J., M. Delgado, G. Bocedi, M. Baguette, K. Bartoń, D. Bonte, I. Boulangeat, J. A. Hodgson, A. Kubisch, V. Penteriani, M. Saastamoinen, V. M. Stevens, and J. M. Bullock. 2013. Dispersal and species' responses to climate change. Oikos 122:1532–1540.

Van der Stocken, T., D. Carroll, D. Menemenlis, M. Simard, and N. Koedam. 2019a. Global-scale dispersal and connectivity in mangroves. Proc. Natl. Acad. Sci. 116:915–922.

Van der Stocken, T., B. Vanschoenwinkel, D. Carroll, K. C. Cavanaugh, and N. Koedam. 2022. Mangrove dispersal disrupted by projected changes in global seawater density. Nat. Clim. Chang. 12:685–691. Springer US.

Van der Stocken, T., A. K. S. Wee, D. J. R. De Ryck, B. Vanschoenwinkel, D. A. Friess, F. Dahdouh-Guebas, M. Simard, N. Koedam, and E. L. Webb. 2019b. A general framework for propagule dispersal in mangroves. Biol. Rev. 94:1547–1575.

van Etten, J. 2017. R Package gdistance : distances and routes on geographical grids. J. Stat. Softw. 76.

van Sebille, E. 2014. Adrift.org.au — A free, quick and easy tool to quantitatively study planktonic surface drift in the global ocean. J. Exp. Mar. Bio. Ecol. 461:317–322. Elsevier B.V.

Villarino, E., J. R. Watson, B. Jönsson, J. M. Gasol, G. Salazar, S. G. Acinas, M. Estrada, R. Massana, R. Logares, C. R. Giner, M. C. Pernice, M. P. Olivar, L. Citores, J. Corell, N. Rodríguez-Ezpeleta, J. L. Acuña, A. Molina-Ramírez, J. I. González-Gordillo, A. Cózar, E. Martí, J. A. Cuesta, S. Agustí, E. Fraile-Nuez, C. M. Duarte, X. Irigoien, and G. Chust. 2018. Large-scale ocean connectivity and planktonic body size. Nat. Commun. 9. Springer US.

Wee, A. K. S., A. M. E. Noreen, J. Ono, K. Takayama, P. P. Kumar, H. T. W. Tan, M. N. Saleh, T. Kajita, and E. L. Webb. 2020. Genetic structures across a biogeographical barrier reflect dispersal potential of four Southeast Asian mangrove plant species. J. Biogeogr. 47:1258–1271.

Wee, A. K. S., K. Takayama, T. Asakawa, B. Thompson, Onrizal, S. Sungkaew, N. X. Tung, M. Nazre, K. K. Soe, H. T. W. Tan, Y. Watano, S. Baba, T. Kajita, and E. L. Webb. 2014. Oceanic currents, not land masses, maintain the genetic structure of the mangrove *Rhizophora mucronata* Lam. (Rhizophoraceae) in Southeast Asia. J. Biogeogr. 41:954–964.

Weir, B. S., and C. C. Cockerham. 1984. Estimating f -statistics for the analysis of population structure. Evolution (N. Y). 38:1358–1370.

Wilson, G. A., and B. Rannala. 2003. Bayesian inference of recent migration rates using multilocus genotypes. 1191:1177–1191.

Wu, Z.-Y., J. Liu, J. Provan, H. Wang, C.-J. Chen, M. W. Cadotte, Y.-H. Luo, B. S. Amorim, D.-Z. Li, and R. I. Milne. 2018. Testing Darwin's transoceanic dispersal hypothesis for the inland nettle family (Urticaceae). Ecol. Lett. 21:1515–1529.

Xu, S., Z. He, Z. Zhang, Z. Guo, W. Guo, H. Lyu, J. Li, M. Yang, Z. Du, Y. Huang, R. Zhou, C. Zhong, D. E. Boufford, M. Lerdau, C. I. Wu, N. C. Duke, S. Shi, S. Y. Lee, X. Li, Y. Yang, X. Wang, Y. Chen, S. Yang, Y. Hou, T. Tang, W. L. Ng, L. Chi, W. Zhao, J. Ruan, Q. Li, W. Wang, L. Chen, G. Lin, B. Liao, A. Wee,

M. Muehlenberg, M. Sun, K. Kathiresan, R. E. Prabowo, T. Kajita, A. Amir, J. Yong, L. P. Jayatissa, H. J. Lin, P. C. Liao, S. Havanond, C. Cannon, K. Krauss, E. Proffitt, D. Devlin, E. A. Hungate, and R. T. Baereleo. 2017. The origin, diversification and adaptation of a major mangrove clade (Rhizophoreae) revealed by whole-genome sequencing. Natl. Sci. Rev. 4:721–734.

Xuereb, A., L. Benestan, É. Normandeau, R. M. Daigle, J. M. R. Curtis, L. Bernatchez, and M.-J. Fortin. 2018. Asymmetric oceanographic processes mediate connectivity and population genetic structure, as revealed by RADseq, in a highly dispersive marine invertebrate (*Parastichopus californicus*). Mol. Ecol. 27:2347–2364.

Supplementary Material

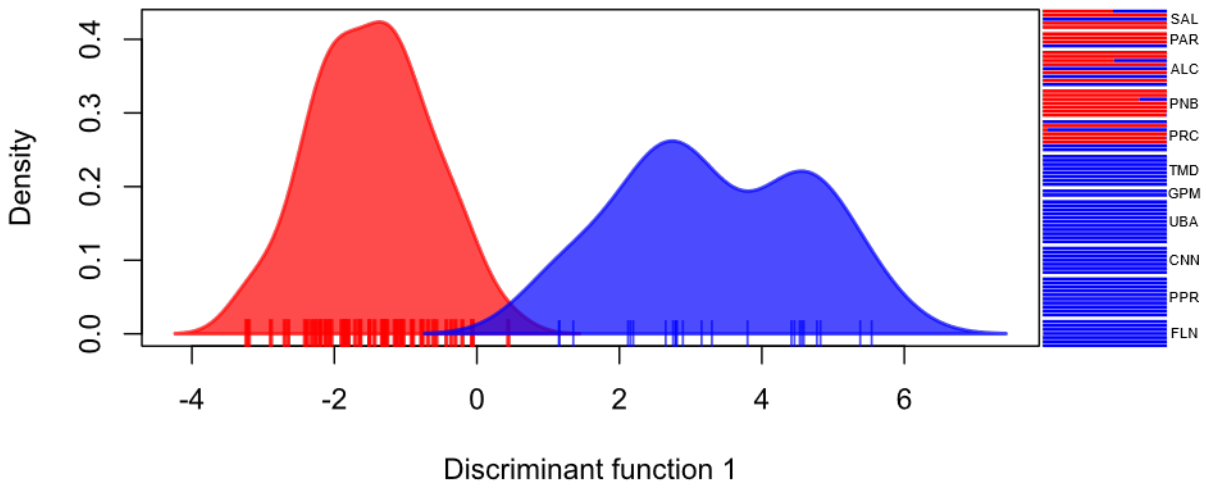

Supplementary Figure 1. Genetic structure of *R. mangle* revealed by discriminant analysis of principal components. Left panel: individual density plot of the first discriminant function (K = 2). Right panel: DAPC-based clustering at individual level, in which lines denotes individuals. In both panels, colors represent assigned clusters. Acronyms for sampling sites follows Table 1.

Supplementary Information 1. Panmixia evolutionary scenario for the inference of migration rates with the software fastsimcoal26.

```
//Parameters for the coalescence simulation program : fastsimcoal.exe
13 samples to simulate :
//Population effective sizes (number of genes)
1000
1000
1000
1000
1000
1000
1000
1000
1000
1000
1000
20000000
20000000
//Samples sizes and samples age
20
20
20
20
20
20
20
20
20
20
20
0 T1
0 T2
//Growth rates    : negative growth implies population expansion
0
0
0
0
0
0
0
0
0
0
0
0
0
//Number of migration matrices : 0 implies no migration between demes
3
//Migration matrix 0
0 M0I M02 M03 M04 0 0 0 0 0 0 0 0
MI0 0 MI2 MI3 MI4 0 0 0 0 0 0 0 0
M20 M2I 0 M23 M24 0 0 0 0 0 0 0 0
M30 M3I M32 0 M34 0 0 0 0 0 0 0 0
M40 M4I M42 M43 0 0 0 0 0 0 0 0 0
0 0 0 0 0 0 M56 M57 M58 M59 M510 0 0
```

```
0 0 0 0 0 M65 0 M67 M68 M69 M610 0 0
0 0 0 0 0 M75 M76 0 M78 M79 M710 0 0
0 0 0 0 0 M85 M86 M87 0 M89 M810 0 0
0 0 0 0 0 M95 M96 M97 M98 0 M910 0 0
0 0 0 0 0 M105 M106 M107 M108 M109 0 0 0
0 0 0 0 0 0 0 0 0 0 0 0
0 0 0 0 0 0 0 0 0 0 0 0
//Migration matrix 1
0 M0I M02 M03 M04 0 0 0 0 0 0 0
MI0 0 MI2 MI3 MI4 0 0 0 0 0 0 0
M20 M2I 0 M23 M24 0 0 0 0 0 0 0
M30 M3I M32 0 M34 0 0 0 0 0 0 0
M40 M4I M42 M43 0 0 0 0 0 0 0 0
0 0 0 0 0 0 0 0 0 0 0 0
0 0 0 0 0 0 0 0 0 0 0 0
0 0 0 0 0 0 0 0 0 0 0 0
0 0 0 0 0 0 0 0 0 0 0 0
0 0 0 0 0 0 0 0 0 0 0 0
0 0 0 0 0 0 0 0 0 0 0 0
0 0 0 0 0 0 0 0 0 0 0 0
0 0 0 0 0 0 0 0 0 0 0 0
//Migration matrix 2
0 0 0 0 0 0 0 0 0 0 0 0
0 0 0 0 0 0 0 0 0 0 0 0
0 0 0 0 0 0 0 0 0 0 0 0
0 0 0 0 0 0 0 0 0 0 0 0
0 0 0 0 0 0 0 0 0 0 0 0
0 0 0 0 0 0 0 0 0 0 0 0
0 0 0 0 0 0 0 0 0 0 0 0
0 0 0 0 0 0 0 0 0 0 0 0
0 0 0 0 0 0 0 0 0 0 0 0
0 0 0 0 0 0 0 0 0 0 0 0
0 0 0 0 0 0 0 0 0 0 0 0
0 0 0 0 0 0 0 0 0 0 0 0
0 0 0 0 0 0 0 0 0 0 0 0
//historical event: time, source, sink, migrants, new deme size, new growth rate,
migration matrix index
13 historical event
T1 5 11 1 1 0 1
T1 6 11 1 1 0 1
T1 7 11 1 1 0 1
T1 8 11 1 1 0 1
T1 9 11 1 1 0 1
T1 10 11 1 1 0 1
T1 11 11 0 0.0001 0 1
T2 0 12 1 1 0 2
T2 1 12 1 1 0 2
T2 2 12 1 1 0 2
T2 3 12 1 1 0 2
T2 4 12 1 1 0 2
T3 11 12 1 1 0 2
//Number of independent loci [chromosome]
1 0
//Per chromosome: Number of contiguous linkage Block: a block is a set of contiguous
loci
```

```
1
//per Block:data type, number of loci, per generation recombination and mutation
rates and optional parameters
FREQ 1 0 2.5e-8

// Priors and rules file
// *********************

[PARAMETERS]
//#isInt? #name   #dist.#min  #max
//all Ns are in number of haploid individuals
0  M0I         logunif  0.00001  0.1     output
0  M02         logunif  0.00001  0.1     output
0  M03         logunif  0.00001  0.1     output
0  M04         logunif  0.00001  0.1     output
0  MI0         logunif  0.00001  0.1     output
0  MI2         logunif  0.00001  0.1     output
0  MI3         logunif  0.00001  0.1     output
0  MI4         logunif  0.00001  0.1     output
0  M20         logunif  0.00001  0.1     output
0  M2I         logunif  0.00001  0.1     output
0  M23         logunif  0.00001  0.1     output
0  M24         logunif  0.00001  0.1     output
0  M30         logunif  0.00001  0.1     output
0  M3I         logunif  0.00001  0.1     output
0  M32         logunif  0.00001  0.1     output
0  M34         logunif  0.00001  0.1     output
0  M40         logunif  0.00001  0.1     output
0  M4I         logunif  0.00001  0.1     output
0  M42         logunif  0.00001  0.1     output
0  M43         logunif  0.00001  0.1     output
0  M56         logunif  0.00001  0.1     output
0  M57         logunif  0.00001  0.1     output
0  M58         logunif  0.00001  0.1     output
0  M59         logunif  0.00001  0.1     output
0  M510        logunif  0.00001  0.1     output
0  M65         logunif  0.00001  0.1     output
0  M67         logunif  0.00001  0.1     output
0  M68         logunif  0.00001  0.1     output
0  M69         logunif  0.00001  0.1     output
0  M610        logunif  0.00001  0.1     output
0  M75         logunif  0.00001  0.1     output
0  M76         logunif  0.00001  0.1     output
0  M78         logunif  0.00001  0.1     output
0  M79         logunif  0.00001  0.1     output
0  M710        logunif  0.00001  0.1     output
0  M85         logunif  0.00001  0.1     output
0  M86         logunif  0.00001  0.1     output
0  M87         logunif  0.00001  0.1     output
0  M89         logunif  0.00001  0.1     output
0  M810        logunif  0.00001  0.1     output
0  M95         logunif  0.00001  0.1     output
0  M96         logunif  0.00001  0.1     output
0  M97         logunif  0.00001  0.1     output
0  M98         logunif  0.00001  0.1     output
```

```
0  M910        logunif  0.00001  0.1     output
0  M105        logunif  0.00001  0.1     output
0  M106        logunif  0.00001  0.1     output
0  M107        logunif  0.00001  0.1     output
0  M108        logunif  0.00001  0.1     output
0  M109        logunif  0.00001  0.1     output
1  T1          unif     10       20000   output
1  T2          unif     10       20000   output
1  T3          unif     10       20000   output

[RULES]

T3 > T2
T2 > T1
```

Supplementary Information 2. Steppingstone evolutionary scenario for the inference of migration rates of the north group with the software fastsimcoal26. A similar scenario, considering one more population, was used for the analysis of the south group.

```
//Parameters for the coalescence simulation program : fastsimcoal.exe
6 samples to simulate :
//Population effective sizes (number of genes)
1000
1000
1000
1000
1000
20000000
//Samples sizes and samples age
20
20
20
20
20
0 T1
//Growth rates    : negative growth implies population expansion
0
0
0
0
0
0
//Number of migration matrices : 0 implies no migration between demes
2
//Migration matrix 0
0        M0I      0        0        0        0
MI0      0        MI2      0        0        0
0        M2I      0        M23      0        0
0        0        M32      0        M34      0
0        0        0        M43      0        0
0        0        0        0        0        0
//Migration matrix 1
0        0        0        0        0        0
0        0        0        0        0        0
0        0        0        0        0        0
0        0        0        0        0        0
0        0        0        0        0        0
0        0        0        0        0        0
//historical event: time, source, sink, migrants, new deme size, new growth rate,
migration matrix index
5 historical event
T1 0 5 1 1 0 1
T1 1 5 1 1 0 1
T1 2 5 1 1 0 1
T1 3 5 1 1 0 1
T1 4 5 1 1 0 1
//Number of independent loci [chromosome]
1 0
//Per chromosome: Number of contiguous linkage Block: a block is a set of contiguous
loci
1
```

```
//per Block:data type, number of loci, per generation recombination and mutation
rates and optional parameters
FREQ 1 0 2.5e-8

// Priors and rules file
// *********************

[PARAMETERS]
//#isInt? #name   #dist.#min  #max
//all Ns are in number of haploid individuals
0  M0I         logunif  0.00001  0.1     output
0  MI0         logunif  0.00001  0.1     output
0  MI2         logunif  0.00001  0.1     output
0  M2I         logunif  0.00001  0.1     output
0  M23         logunif  0.00001  0.1     output
0  M32         logunif  0.00001  0.1     output
0  M34         logunif  0.00001  0.1     output
0  M43         logunif  0.00001  0.1     output
1  T1          unif           10       20000   output
```

Supplementary Information 3. Directional migration evolutionary scenario for the inference of migration rates of the north group with the software fastsimcoal26. A similar scenario, considering one more population, was used for the analysis of the south group.

```
//Parameters for the coalescence simulation program : fastsimcoal.exe
6 samples to simulate :
//Population effective sizes (number of genes)
1000
1000
1000
1000
1000
20000000
//Samples sizes and samples age
20
20
20
20
20
0 T1
//Growth rates    : negative growth implies population expansion
0
0
0
0
0
0
//Number of migration matrices : 0 implies no migration between demes
2
//Migration matrix 0
0        M0I      M02      M03      M04      0
MI0      0        MI2      MI3      MI4      0
M20      M2I      0        M23      M24      0
M30      M3I      M32      0        M34      0
M40      M4I      M42      M43      0        0
0        0        0        0        0        0
//Migration matrix 1
0        0        0        0        0        0
0        0        0        0        0        0
0        0        0        0        0        0
0        0        0        0        0        0
0        0        0        0        0        0
0        0        0        0        0        0
//historical event: time, source, sink, migrants, new deme size, new growth rate,
migration matrix index
5 historical event
T1 0 5 1 1 0 1
T1 1 5 1 1 0 1
T1 2 5 1 1 0 1
T1 3 5 1 1 0 1
T1 4 5 1 1 0 1
//Number of independent loci [chromosome]
1 0
//Per chromosome: Number of contiguous linkage Block: a block is a set of contiguous
loci
1
```

```
//per Block:data type, number of loci, per generation recombination and mutation
rates and optional parameters
FREQ 1 0 2.5e-8

// Priors and rules file
// *********************

[PARAMETERS]
//#isInt? #name   #dist.#min  #max
//all Ns are in number of haploid individuals
0  M0I         logunif  0.000001  0.01     output
0  M02         logunif  0.000001  0.01     output
0  M03         logunif  0.000001  0.01     output
0  M04         logunif  0.000001  0.01     output
0  MI0         logunif  0.00001  0.1     output
0  MI2         logunif  0.000001  0.01     output
0  MI3         logunif  0.000001  0.01     output
0  MI4         logunif  0.000001  0.01     output
0  M20         logunif  0.00001  0.1     output
0  M2I         logunif  0.00001  0.1     output
0  M23         logunif  0.000001  0.01     output
0  M24         logunif  0.000001  0.01     output
0  M30         logunif  0.00001  0.1     output
0  M3I         logunif  0.00001  0.1     output
0  M32         logunif  0.00001  0.1     output
0  M34         logunif  0.000001  0.01     output
0  M40         logunif  0.00001  0.1     output
0  M4I         logunif  0.00001  0.1     output
0  M42         logunif  0.00001  0.1     output
0  M43         logunif  0.00001  0.1     output
1  T1          unif     10       20000     output

[RULES]
MI0 > M0I
M20 > M02
M30 > M03
M40 > M04
M2I > MI2
M3I > MI3
M4I > MI4
M32 > M23
M42 > M24
M43 > M34
```